Int. Assoc. Sedimentol. Spec. Publ (2018) **48**, 149–172.

An exhumed fine-grained meandering channel in the lower Permian Clear Fork Formation, north-central Texas: Processes of mud accumulation and the role of vegetation in channel dynamics

SHARANE S.T. SIMON[†*], MARTIN R. GIBLING[†], WILLIAM A. DIMICHELE[‡], DAN S. CHANEY[‡] and REBECCA KOLL[§]

[†] *Department of Earth Sciences, Dalhousie University, Halifax, Nova Scotia, Canada*
[‡] *Department of Paleobiology, National Museum of Natural History, Smithsonian Institution, Washington, DC, USA*
[§] *Florida Museum of Natural History, University of Florida, Gainesville, FL, USA*
** Corresponding author: Department of Geology, Allegheny College, Meadville, PA, USA*

ABSTRACT

Ancient fine-grained meandering channels are under-represented in the literature and their formative processes are rarely explored. The Montgomery Ranch 3 site of the Clear Fork Formation of Texas contains an exhumed fine-grained point bar that migrated for at least 50 m within a channel 2 m deep and 36 m wide. The point bar comprises thick inclined layers of unstratified mudstone intercalated with thin layers of fine-grained, ripple cross-laminated sandstone, with dips averaging nearly 16°. Rill casts and swept ripples on the sandstone surfaces indicate declining water levels. Petrographic analysis of the mudstone shows silt and clay laid down from suspension, but sand-sized mud aggregates transported as bedload (present at other sites in the formation) were not observed. The sandstone beds are attributed to lateral accretion on the point bar during periods of sustained flow, whereas the mudstone beds are attributed to oblique accretion as fine sediment draped the bar during waning and low-flow periods. Sandstone and mudstone units are composite units from numerous flow events and their alternation may reflect secular variation in flood frequency and intensity. In an associated abandoned-channel fill, weakly laminated mudstone with desiccation cracks contains leaves and seeds of *Evolsonia texana*, marattialean foliage and *Taeniopteris* sp., with root traces penetrating the leaves. Some taxa preferred high water tables and humid conditions, whereas others were dryland colonisers. This apparent discrepancy may reflect the persistence of wetter channel reaches within an otherwise dry setting. Despite the scarcity of preserved plant fossils, vegetation was probably sufficiently widespread to promote bank strength and local sediment accumulation.

Keywords: Exhumed point bar, fine-grained meandering channels, oblique accretion, lateral accretion, vegetation

INTRODUCTION

Fine-grained deposits laid down in meandering-fluvial channels are common in the geological record (Stewart, 1981; Edwards *et al.*, 1983; Thomas *et al.*, 1987; Mack *et al.*, 2003; Ghosh *et al.*, 2006; Rygel & Gibling, 2006; Simon & Gibling, 2017a; Dasgupta *et al.*, 2017). They have received less attention than sand-rich deposits, which are as economically important as hydrocarbon

Fluvial Meanders and Their Sedimentary Products in the Rock Record, First Edition.
Edited by Massimiliano Ghinassi, Luca Colombera, Nigel P. Mountney and Arnold Jan H. Reesink.

reservoirs and aquifers. Due to the erodible nature of the strata, cliff exposures are uncommon and exhumed channels and bars suitable for high-resolution architectural analysis represent an unusual opportunity to explore the processes responsible for their formation.

Among outstanding issues pertaining to fine-grained meandering systems, two are highlighted in this paper. Firstly, a thorough interpretation depends on discriminating between the processes that deposit fine sediment. Within active channels, these processes include lateral accretion of sand-sized mud aggregates transported as bedload (Rust & Nanson, 1989), oblique accretion of mud from suspension on bars and banks (Page *et al.*, 2003) and counter point bar accretion in the downstream parts of meander bends (Smith *et al.*, 2009). Discriminating mud deposited as bedload (lateral accretion) from mud deposited from suspension (oblique accretion) leads to an interpretation of active flow conditions or quiescence – a fundamental distinction in channel behaviour. Distinguishing these processes in the geological record is difficult because 1) they form end-members in a depositional spectrum, 2) desiccation and pedogenesis may destroy evidence of surface processes; and 3) diagenesis may preferentially alter the finer sediment (Sambrook Smith *et al.*, 2016; Simon & Gibling, 2017a,b). Criteria for discriminating between in-channel processes of mud deposition are addressed in the following section. Mud may also be deposited from suspension and as bedload aggregates on floodplains and from suspension in abandoned channels.

Secondly, many fine-grained fluvial deposits show features indicative of seasonal flow and periodic dryness, which allowed rooted vegetation to become established in the channel. Fielding *et al.* (2009) used in-channel vegetation as a criterion to identify tropical, seasonal fluvial systems in the ancient record. However, plants are typically poorly preserved in dryland fluvial deposits, leading to possibly erroneous conclusions that vegetation was sparse or absent. Where plant fossils are present within channel deposits, analysis of taxonomy and palaeoecology is crucial in establishing the capability of the vegetation to influence channel dynamics, as documented in many modern rivers (e.g. Millar, 2000; Eaton & Giles, 2009; Edmaier *et al.*, 2011). More analysis is required to supplement the modest number of existing studies for the ancient record (e.g. Demko *et al.*, 1998; Fielding & Alexander, 2001; Bashforth *et al.*, 2014; Ielpi *et al.*, 2015).

In the early Permian Clear Fork Formation of Texas, Simon & Gibling (2017a) documented fine-grained channel deposits exposed in low cliffs and exhumed on flat-lying ground. The inclined strata include layers rich in sand-sized mud aggregates and in silt and clay, allowing an assessment of accretion processes; and some localities have yielded exceptionally well-preserved plant fossils. Data from three localities at a similar stratigraphic level on Montgomery Ranch (MR1, MR2 and MR3) were included in these earlier analyses. The MR3 locality, documented in detail here, received additional study because 1) an exhumed channel body exposes inclined strata, the fill of an abandoned channel and the adjacent channel margin, allowing unusual certainty in reconstructing the channel geometry and accretion processes; and 2) an unusual and well-preserved assemblage of gigantopterids, marattialeans tree ferns and *Taenopteris*, as well as root traces, allows an assessment of habitat and the contribution of the vegetation to fluvial dynamics.

The integration of new information from MR3 with data from MR1 and MR2 contributes to addressing a central question: what processes govern sediment accumulation and morphodynamics in fine-grained meandering channels?

MUD ACCUMULATION IN ACTIVE FLUVIAL CHANNELS

As set out in Table 1, three main processes of mud accumulation have been recognised in active channels. Lateral accretion involves deposition of bedload on point bars during active flow (Jackson, 1981; Rust & Nanson, 1989; Sambrook Smith *et al.*, 2015). In contrast, oblique accretion involves deposition of suspended load on steep accretionary banks and bars during low-energy and waning flow (Page *et al.*, 2003). The former process is familiar from perennial rivers around the world and in seasonal rivers with a moderate duration of annual flow. The latter process has been documented from strongly seasonal channels where near-bankfull conditions are achieved with moderate to low flow strength. During waning flow, fine sediment drapes the progressively exposed banks and may extend to the channel floor if flow in the channel ceases entirely.

Table 1. Comparison of lateral accretion, oblique accretion and counter point bar accretion in modern, sinuous fine-grained channels, in terms of processes and deposits.

	Fine-grained Deposits of Modern Sinuous Channels		
	Lateral-Accretion Deposits	Oblique-Accretion Deposits	Counter Point Bar Deposits
Processes	Bedload deposits predominate, laid down on a migrating point bar during relatively prolonged flow in the channel. Point-bar advance commonly matches cutbank retreat. Relatively rapid rate of migration.	Suspended-load deposits predominate, draped on a prograding accretionary bank during low-energy and waning flow, commonly as banks are exposed. Accretion may narrow channel if cutbank erodes slowly. Relatively slow rate of migration.	Bed-load and suspended-load deposits laid down in the downstream parts of point bars that are migrating downvalley. Commonly subject to reverse eddy currents with upstream flow vectors.
Sediment	Coarser sand and sand-sized, pedogenic mud aggregates. Aggregates washed into channels from floodplains and banks.	Fine sand, silt and clay, commonly interbedded.	Silt predominant, with modest proportions of sand and minimal clay.
Structures and features	Trough and planar cross-beds, ripple cross-lamination, rare plane beds, erosion surfaces. Bedforms commonly directed up the inclined surfaces due to helicoidal flow. Upward fining to floodplain deposits.	Ripple cross-lamination (bedforms may be scarce), desiccation cracks, rill casts, bioturbation. May rest on point-bar deposits lower in the channel. Overlain by floodplain deposits.	Ripple cross-lamination, commonly climbing, and horizontal lamination.
Inclined surfaces	Dips modest, commonly < 10°, 4 to 15° in sandy and silty point bars (Allen, 1970; Sambrook Smith *et al.*, 2015) and 10 to 15° in muddy point bars (Jackson, 1981).	Dips steep, locally as high as 29° (Page *et al.*, 2003) and 30 to 40° (Brooks, 2003a). Sharp decrease in dip (oblique contact) of inclined surfaces on point bar or channel base.	Dips relatively steep, 16° and 22° in two examples (Smith *et al.*, 2009). Concave planforms on bar surfaces.
Vegetation	Plant material with bedload, rooted vegetation rare but present locally.	Plant debris common in fine drapes. Rooted vegetation commonly established low in channel during exposure.	Plant debris common.
Modern examples	Jackson, 1981; Sambrook Smith *et al.*, 2015 (for point-bars in general: Allen, 1970; Jackson, 1976; Parker *et al.*, 2011).	Bluck, 1971; Taylor & Woodyer, 1978; Nanson & Croke, 1992; Page *et al.*, 2003; Brooks, 2003a, b.	Woodyer, 1975; Hickin, 1979, Page & Nanson, 1982; Nanson & Page, 1983; Makaske & Weerts, 2005; Smith *et al.*, 2009.

For mud deposits in the geological record, criteria for discriminating between these processes include grain-size and type, the range of sedimentary features, the dip of inclined surfaces and the presence or absence of rooted vegetation low in the channel (Table 1). An important criterion is the presence or absence of sand-sized mud aggregates derived from reworking of palaeosols, a prominent bedload component in many distal dryland settings (Rust & Nanson, 1989; Maroulis & Nanson, 1996). Although cryptic bedforms may be observed in mudstone outcrops (Èkes, 1993), aggregate identification usually requires petrographic analysis and imaging of these difficult materials (Müller *et al.*, 2004; Wolela & Gierlowski-Kordesch, 2007; Gastaldo *et al.*, 2013; Dasgupta *et al.*, 2017; Simon & Gibling, 2017b).

Mud may also accumulate in the downstream parts of meander bends through counter point bar accretion. Based on examples in the Peace River

of Canada and elsewhere, diagnostic criteria (Table 1) include strata with a geometry that is concave to the adjacent channel, the predominance of ripple cross-laminated silt, modest sand, minimal clay and the relatively steep dips of inclined beds.

TECTONIC AND STRATIGRAPHIC SETTING

The Clear Fork Formation of Kungurian age was deposited on the Eastern Shelf of the Midland Basin, between 0° and 5° N of the equator on the western coastal zone of Pangea (Fig. 1A; Ziegler *et al.*, 1997; Scotese, 1999). The formation was deposited by rivers that flowed generally to the west, recycling Pennsylvanian deposits with contributions from the denuded Wichita, Arbuckle and Ouachita mountains (King, 1937; Oriel *et al.*, 1967; Houseknecht, 1983). During the early Permian, tectonic quiescence prevailed with intermittent strike-slip movement along the Matador and Red River uplifts (Regan & Murphy, 1986; Budnik, 1989; Brister *et al.*, 2002).

The Clear Fork Formation is conformably underlain by the Leuders Formation, a tidal deposit intercalated with marine carbonates (DiMichele *et al.*, 2006). The formation is conformably overlain by the San Angelo Formation of the Pease River Group, consisting of sandy fluvial deposits and muddy coastal-plain deposits (Nelson & Hook, 2005). Burial depth may not have exceeded 1100 m based on regional stratigraphic considerations and maturation data from Eastern Shelf strata (Bein & Land, 1983; Hackley *et al.*, 2009; Simon & Gibling, 2017a).

In the non-marine outcrop areas of the Clear Fork Formation in north-central Texas, the formation is 350 to 365 m-thick and is informally subdivided into lower, middle and upper units (Fig. 1B; Nelson *et al.*, 2013). The formation comprises fluvial and playa-lake deposits of red mudstone with subordinate sandstone, carbonate and evaporate; and the beds are nearly horizontally disposed with WNW dips of less than 1° (Olson, 1958; Wardlaw, 2005; Nelson *et al.*, 2013). Interestingly and unusually, many meandering-channel bodies are exhumed at the land surface (Edwards *et al.*, 1983; Simon & Gibling, 2017a). Fossils include seed plants, vertebrates and trackways of tetrapods and myriapods (Romer, 1928; Olson, 1958; Murry & Johnson, 1987; DiMichele *et al.*, 2006; Chaney & DiMichele, 2007; Anderson *et al.*, 2008; Lucas *et al.*, 2011; Milner & Schoch, 2013).

Based on regional studies across Euramerica (Tabor & Poulsen, 2008; Tabor, 2013), the western equatorial region of Pangea experienced semi-arid to arid conditions with seasonal precipitation. For the Clear Fork Formation (Tabor & Montañez, 2004; DiMichele *et al.,* 2006; Chaney & DiMichele, 2007; Simon, 2016), conditions became drier upsection, as shown by 1) an increased abundance of pedogenic carbonate and evaporite, with bedded dolomite and gypsum in the upper unit; 2) an upward change in cement and nodule composition from calcite, ankerite and dolomite in the lower and middle units to dolomite, gypsum and celestine in the upper unit; 3), a decrease in the proportion of channel bodies and increase of playa-lake deposits upwards; and 4) an upward disappearance of plant and vertebrate fossils, with the uppermost known occurrences just above the Burnet Dolomite.

Fig. 1. (A) Permo–Pennsylvanian palaeogeography of north-central Texas, showing the main uplifts and basin areas (modified from Tabor & Montañez, 2004). The study area is located in the Eastern Shelf and indicated by the pink box. (B) Composite log of the Clear Fork Formation along the Wichita River, showing the occurrence and relative thickness of the main channel bodies studied (modified from Nelson *et al.*, 2013). The Montgomery Ranch 3 (MR3) study site is located in the upper Clear Fork Formation. (C) Planform exposure of an exhumed point bar at MR3 with resistant, discontinuous sandstone scarps formed by inclined beds, abandoned channel, channel margin (cutbank) and adjacent floodplain deposits, visible on Google Earth (red arrow shows north). Yellow lines with triangles represent scarp strike and dip direction, respectively. The two scarps that dip north (green lines) are part of an underlying channel body. Rose diagram represents palaeoflow for all inclined surfaces based on ridge-and-furrow structures that represent cross-lamination. The blue lines and dots indicate the location of subsequent figures. Inset map shows the location of the three Montgomery Ranch sites. [MR1: 33°49'50.84″N, 99°37'35.55″W; MR2: 33°49'34.15″N, 99°37'43.42″W; MR3: 33°50'8.08″N, 99°37'5.28″W]. (D) Log of sandstone and mudstone units as measured in a strike exposure of inclined beds (element LA). (E) Log of mudstone unit underlying the exhumed point bar. On D and E, sand sizes are shown by VF, F and M (very fine, fine and medium, respectively).

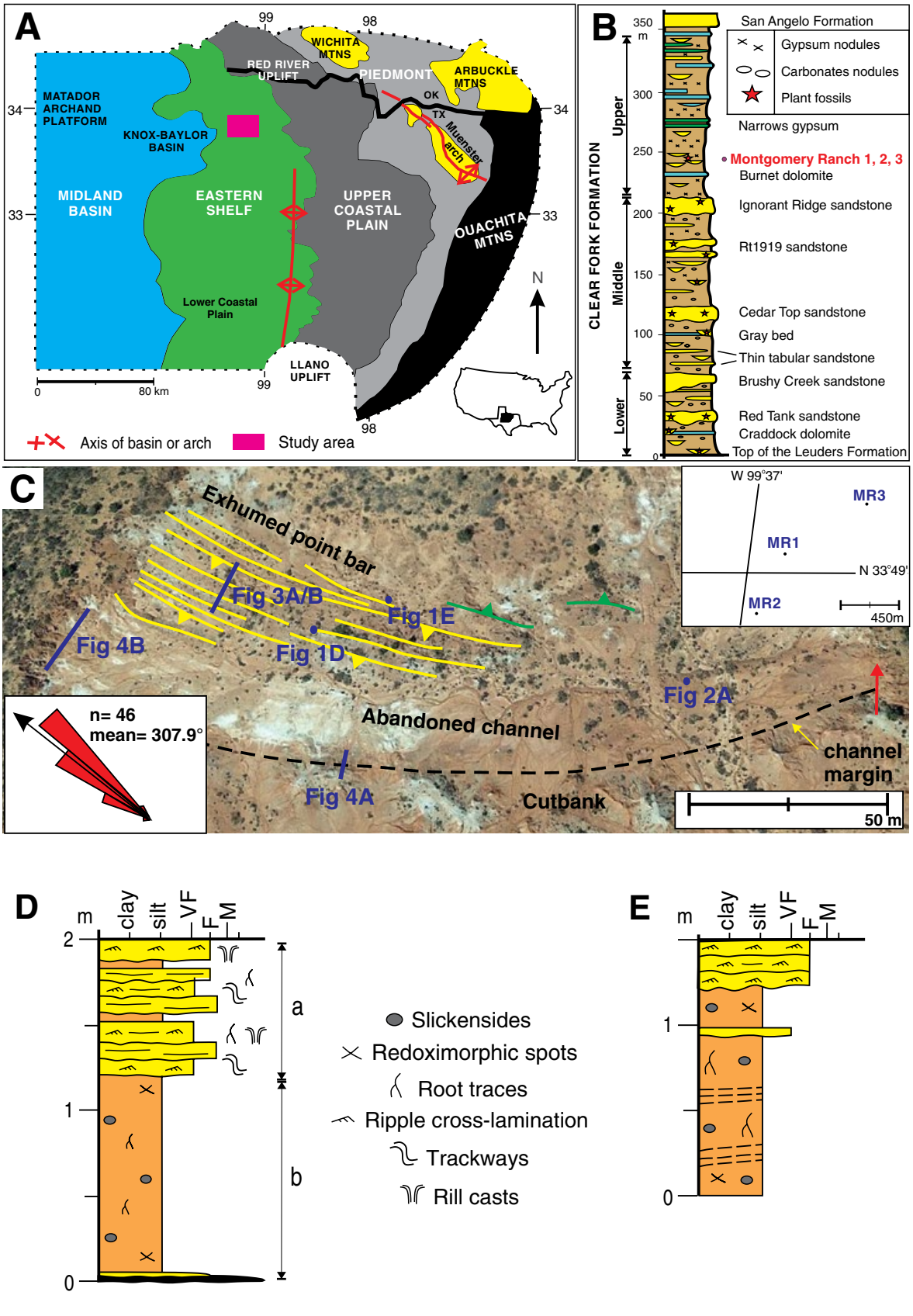

Fig. 1. (Continued)

Nelson *et al.* (2013) mapped the upper Clear Fork as a unit 165 m-thick, composed of mudstone and claystone with thin layers of siltstone and very fine-grained sandstone. Gypsum is abundant as nodules and beds, locally interlayered with dolomite and mudstone. Palaeosols are weakly developed. The study locality of Montgomery Ranch 3 (MR3) is one of three studied sites (other sites: MR1 and MR2) in the upper unit, approximately 1.5 km apart and within a stratigraphic range of less than 50 m (Fig. 1B and C). In view of the low dip, the precise stratigraphic relationship of the sites is difficult to ascertain. Exhumed accretion deposits are quartz-rich at MR2 and variably mud-rich and quartz-rich at MR1 and MR3 (Simon & Gibling, 2017a). Despite their proximity in time and space on the Permian landscape, these channel bodies show key differences that are discussed below.

METHODS

The MR3 locality was evaluated over two field seasons as part of a broader study of fluvial sites. Located in Foard County, the outcrops comprise partially exposed channel components with exhumed surfaces and cliff faces oriented parallel and perpendicular to local flow and they extend for 216 m across two hectares (Fig. 1C). Three elements were recognised: channel-base deposits (CD), inclined strata (LA) and massive mudstone (MM); formal element names are in italics where used in the later text (Table 2). Plant fossils were excavated from four sites at the locality.

To reconstruct the exhumed surfaces, eroded ridges up to 10 m-long formed by inclined sandstone bedsets were mapped using GPS readings accurate to ± 3 m. Depending on ridge length, at

Table 2. Elements for meandering-channel deposit at the MR3 site in the Clear Fork Formation. Facies codes from Miall (1996). Redoximorphic spots and Fe-oxide staining are prominent in all facies, which are red, brown and grey. Plants include woody fragments and leaves with *Diplichnites gouldi* trackways. VF and F = very fine and fine sand, respectively. Gm: massive or crudely bedded pebble conglomerate; Sr: ripple cross-laminated sandstone; Fl: finely laminated mudstone; Fm: massive to weakly ripple-cross laminated mudstone. A = abundant, C = common, R = rare.

Elements	Grain-size	Sedimentary features and fossils	Petrography	Interpretation
Channel-base deposits (CD)	Cemented siltstone, pebble conglomerate, VF-F sandstone.	Gm, Sr as lenses and mounds. Up to 0.3 m-thick.	Pebbles of finely crystalline dolomite, silt-sized quartz, and clay.	Basal cemented deposits laid down during or after incision; clasts reworked from local palaeosols.
Inclined strata (LA)	Bedsets of a) structureless to weakly ripple cross-laminated mudstone; and b) VF-F sandstone.	Sr, Fm. Climbing, swept, starved and symmetrical ripples; rill casts, trackways (R), root traces (R). Mudstone units < 1.5 m-thick and sandstone units < 0.4 m-thick.	Quartzose grains in clay and hematite matrix, with dolomite cement.	Lateral and oblique accretion deposits formed in a point bar. Bedload transport of sand-sized quartzose grains with suspension drapes on steep surfaces. Lower flow regime, with erosive flood events. Locally vegetated.
Massive mudstone (MM)	Weakly laminated to structureless mudstone, with some VF sandstone lenses.	Sr, Fl, Fm, red-brown to grey. Mud cracks, slickensides, charcoal, peds with clay coats, clastic dykes, mud chips. Plants (C), seeds (R), root traces (R to C), coprolites (R), bivalves (R). Up to 3 m-thick.	Quartzose grains in clay and hematite matrix, with dolomite cement.	Floodplain deposits and abandoned-channel fill with incipient to moderately developed soils. Low-energy flows and suspension settling. Modification due to exposure. Plants from vegetation growing in channel and riparian zone.

least three readings (upstream, medial and downstream sites) were recorded, encompassing grain-size and sedimentary features, strike/dip and palaeoflow. Using a tape or a rangefinder accurate to ± 1 m, ridge length and the distance between ridge crests were measured as a field check for the GPS. For cliff sections, key stratigraphic surfaces and sedimentological observations were recorded on photomosaics. One vertical profile (Fig. 1D) was measured through exhumed inclined bedsets and a second (Fig. 1E) was measured across a floodplain section adjacent to the channel body. Three fluvial elements were identified and the term 'mudstone' implies varied proportions of clay and silt (Table 1).

The exposure allows the direct measurement of channel-body dimensions. Channel-body thickness was estimated in two ways, as the maximum vertical extent of inclined surfaces and as the thickness of an abandoned-channel fill from the basal contact to the base of the overlying floodplain deposit. Channel width was measured as the orthogonal distance between the last lateral-accretion surface to the north and the onlap of channel fill onto flat-lying floodplain deposits to the south, assuming that abandonment was concurrent with the termination of cutbank retreat. The width shortly before final filling of the channel is represented by the width of the concentric fill seen in a low cliff.

Five unpolished thin sections were examined under plane-polarised light and one polished thin section was studied using SEM/EDS (Scanning Electron Microscopy/Energy-Dispersive X-ray Spectroscopy; Table 3). X-ray diffraction (XRD) analysis was conducted on seven random powder mounts and three of these samples were selected for < 2 µm clay fraction analysis. Details of the sample preparation and analytical techniques are presented in Simon *et al.* (2016). The set includes four samples of massive mudstone, two from inclined strata and one from a channel-base deposit.

FLUVIAL ELEMENTS

Channel-base deposits (CD)

Description: Channel-base deposits consist of cemented siltstone as suites of discontinuous lenses < 15 cm-thick with convex-up tops. The siltstone commonly drapes mounds with a core of red mudstone (MM; Fig. 2A). The mounds have a maximum height and length of 30 cm and 1 m, respectively, with crest-to-crest spacing of 1 to 3 m. The siltstone beds comprise cosets of red and grey cross-lamination with preserved ripple forms, some of which climb at a low angle (Fig. 2B and C). Adjacent to the siltstone is a 3 cm-thick layer of pebble conglomerate composed of carbonate clasts and very fine-grained to fine-grained ripple cross-laminated sandstone. XRD and petrographic analysis shows that the siltstone is

Table 3. Samples from the MR3 field area, with their elements, relative stratigraphic position and analyses conducted.

Sample numbers	Sediment type	Analyses			
		thin section	SEM/ EDS	XRD (bulk)	XRD (<2 µm)
MR3_1	Cemented siltstone bed (CD)	✓	–	✓	–
MR3_2	Structureless mudstone adjacent to the channel body (MM)	–	–	✓	✓
MR3_3	Structureless siltstone in the abandoned-channel fill (MM)	✓	✓	✓	–
MR3_4	Fossiliferous structureless siltstone in the abandoned-channel fill (MM)	✓	–	✓	✓
MR3_5	Cemented ripple-cross laminated sandstone in inclined bedsets of the exhumed point bar (LA)	✓	–	✓	
MR3_6	Structureless mudstone in inclined bedsets of the exhumed point bar (LA)	✓	–	✓	✓
MR3_7	Structureless mudstone underlying the channel body (MM)	–	–	✓	–

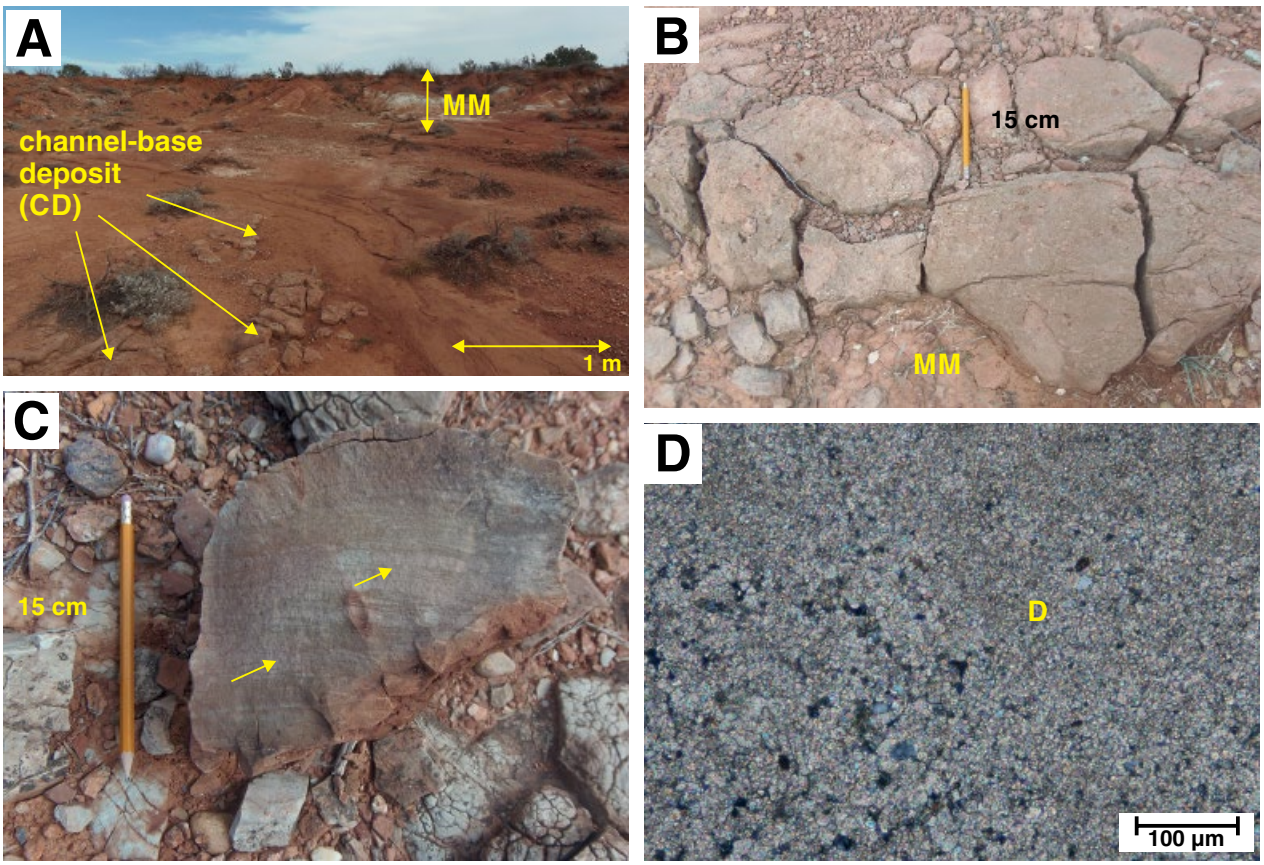

Fig. 2. Channel-base deposits (CD). (A) Channel-base deposits exposed across flatground, at the base of an abandoned channel filled with weakly laminated and structureless mudstone (MM). (B) Thick, structureless cemented siltstone with pebble conglomerate draped over mounds of structureless mudstone (MM), tapering down-current (to the left). (C) Cross-section through the siltstone showing the convex-upward surface and poorly-preserved ripple cross-laminated layers (yellow arrows). (D) Photomicrograph of cemented siltstone under cross-polarised light showing very finely crystalline dolomite 'D' with a few silt-sized quartz grains and a clay matrix.

composed of quartz grains, some clay matrix and very finely crystalline dolomite (Fig. 2D).

Interpretation: Channel-base deposits are interpreted as channel-lag deposits. The siltstone beds are interpreted as linear, flow-parallel mounds that formed by rapid deposition under lower-regime flow, probably downflow from obstacles that were not preserved. The texture of the carbonate clasts closely resembles that of carbonate-bearing palaeosols at other localities in the formation and the clasts are inferred to be pedogenic nodules that were eroded from soils and concentrated at the channel base. The dolomitic clast composition probably reflects early dolomitisation from shallow continental groundwater with an increased Mg/Ca ratio following calcite precipitation in an evaporative setting (Simon & Gibling, 2017a).

Inclined strata (LA)

Description: Inclined strata are heterolithic units (Thomas *et al.*, 1987) of mudstone and sandstone with an average dip of sandstone surfaces of 15.6 ± 2.6° (n = 29) to the south (Figs 1D, 3A and B). Although stratification is poorly developed within the mudstone units, where visible it is parallel to that in the sandstones (Fig. 3C). The inclined units downlap onto coarse channel-base deposits or unstratified mudstone. Exposed in planview with large-scale curvature that is convex towards the cutbank, they form low, discontinuous scarps up to 2 m high, which can be traced across flat ground for up to 100 m along strike into nearby cliff exposures and for more than 50 m in the dip direction (Figs 1C, 3A and B). Exposures are mainly limited to the upper portions of the

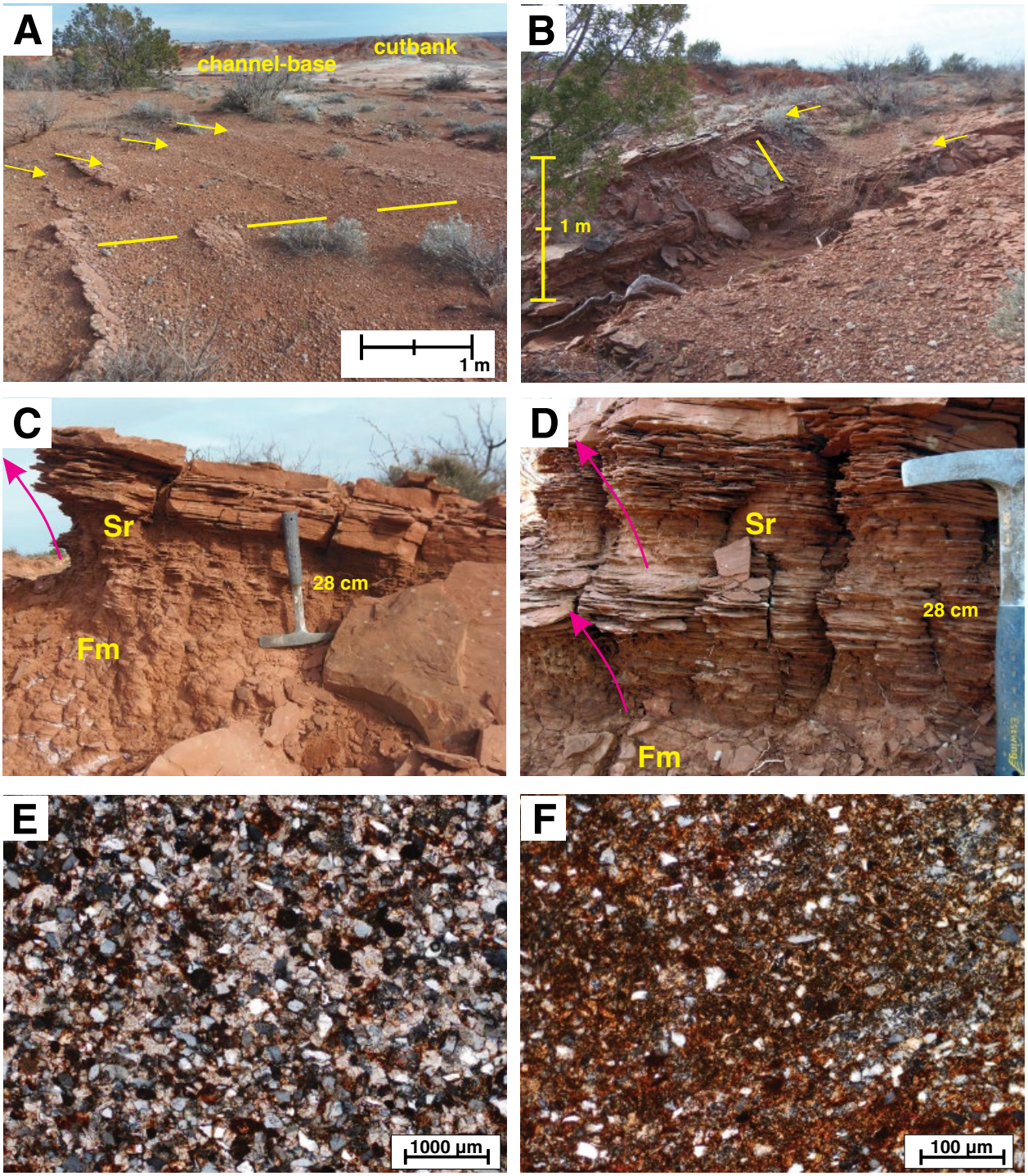

Fig. 3. Inclined strata (LA). (A, B) Planform exposure of resistant, discontinuous sandstone scarps (yellow arrows) interbedded with structureless mudstone (yellow bars). Scarps dip to the right in A and to the left in B, with palaeoflow angled up the inclined surfaces (see rose diagram in Fig. 1C). View in A is southward, across channel-base deposits (white area) to cutbank against older floodplain deposits in distance. (C) Vertical section through scarp. At the base of the sandstone bed, starved ripples are common and ripple sets progressively thicken upward (pink arrow) with less intervening mudstone into a well-developed sandstone layer. The ripple cross-laminated sandstone beds (Sr) dip to the right, overlying a structureless mudstone interval with redoximorphic spots and root traces (Fm). (D) Sandstone bed in the accretion deposits composed of two coarsening-upward beds (pink arrows). (E) Cemented sandstone composed of finely crystalline dolomite with detrital grains and clay matrix. (F) Mudstone composed of silt-sized quartz grains and ferruginous grains in a matrix of hematite and clay.

units. Underlying these strata is a partially exposed, second set of inclined heterolithic strata, which dips to the north with a similar dip angle (green lines on Fig. 1C).

The inclined and well cemented sandstone units are up to 40 cm-thick (mean: 0.25 ± 11 cm). The contacts between the sandstone and mudstone units are mostly gradational (Fig. 3C) but abrupt and erosional in some cases. Starved ripple sets are common in the lowermost, thin-bedded part of the sandstone units and individual beds thicken progressively upward with less intervening mudstone, locally with distinct bedsets that include thickening- and coarsening-upward packages (Fig. 3C and D). The very fine-grained to medium-grained sandstone units are ripple cross-laminated with 2D and rare 3D sets visible as ridge-and-furrow structures. Swept ripple crests are oriented predominantly updip on the inclined surfaces, on average nearly 22° above the horizontal (see Simon & Gibling, 2017a for discussion of swept ripples). Symmetrical ripples and rill casts oriented down-dip are present on bed surfaces. The dip of the inclined sandstone beds varies between adjacent ridges and the most northerly (earliest deposited) inclined bed flattens updip with no convex-up form. Root traces are rarely present, with a few *Diplichnites gouldi* trackways oriented parallel or oblique to the strike of the beds. Based on petrographic analysis, the sandstone is composed of detrital grains and clay cemented by finely crystalline dolomite (Fig. 3E).

The inclined mudstones are up to 1.5 m-thick (mean 1.1 ± 0.3 m) and largely structureless, with poorly-developed slickensides, redoximorphic spots and a few root traces (Fig. 3C). Petrographic analysis shows silt-sized quartz grains in a matrix of hematite and clay (illite, Fe-rich chlorite, kaolinite and mixed-layer clays) with no mud aggregates visible (Fig. 3F). Although aggregates are commonly destroyed during diagenesis, no indication was found of aggregate remnants.

Interpretation: The scarps represent an exhumed point bar with a quasi-complete meander bend and a convex planform. Based on the strike of the ridges and increase in the channel-bend curvature to the south, the point bar mostly migrated by expansion to the south over a distance of 50 m, with no evidence of rotation or translation (Willis, 1989; Ghinassi *et al.*, 2014; Ielpi & Ghinassi, 2014). Like other examples in the Clear Fork Formation, the point bars appear to lack scroll topography (Simon & Gibling, 2017a) based on the absence of convex-up forms at the tops of the most completely preserved sandstones. The presence of a lower set of accretion deposits implies two, vertically stacked point bars, one fully exhumed and another partially exposed.

The sandstones are interpreted as lateral-accretion deposits, laid down as bedload during point-bar migration, with ripples moving laterally along the inclined surfaces. Erosive bases and varying dip angles of the inclined beds represent truncation surfaces (Ghinassi *et al.*, 2014), suggesting that the point bar was eroded during some floods. The earliest deposited sandstone unit on the northern side of the outcrop belt extends from the channel base up an inclined surface and onto the adjacent floodplain, suggesting that bankfull conditions were exceeded shortly after channel accretion commenced. Symmetrical ripples indicate periodic ponding with wind-induced oscillatory flow. Rill casts oriented down the inclined surfaces formed during waning flow as water receded within the channel and near-surface water in the sand drained out. Swept ripples are also attributed to waning flow as ripple crests were stranded on upper levels of the point-bar surfaces but continued to migrate lower down, giving the ripple crests an updip skew (Simon & Gibling, 2017a). The point bar supported arthropods and was vegetated, as indicated by the presence of root traces. The depth to which the water receded is uncertain because the lowest parts of the accretion deposits are not exposed. During shallow burial, the sandstone was cemented with dolomite precipitated from Mg-rich waters.

Based on field and petrographic evidence, the mudstones are interpreted as oblique-accretion deposits, as indicated by the absence of flow structures, mud aggregates and other clasts that could be attributed to transport as bedload. These features collectively suggest deposition from suspension during waning flow or in stagnant water, where sediments draped a steep surface. Similar features are found in modern oblique-accretion deposits (Table 1). Although aggregates were not observed, the mud may have been derived in part from the mechanical wear of mud aggregates during transport (Maroulis & Nanson, 1996).

Within the sandstone units, the presence of stacked bedsets suggests accumulation during several flood events or pulses within a single event. Bedsets are difficult to identify within the mudstone units, but their substantial thickness (up to 1.5 m) suggests that they also contain

multiple bedsets with cryptic boundaries. The commonly gradational contact from mudstone to sandstone units suggests gradually changing depositional conditions, supporting the hypothesis of numerous flow events in each unit. The durations of the units are not known.

Massive mudstone (MM)

Description: Massive mudstone comprises red-brown and grey, weakly laminated to structureless mudstone (Fig. 4A and B). Its principle occurrence is a lenticular sediment body 2 m-thick that onlaps the downdip side of inclined strata on the northern side of the outcrop belt and a steeply-dipping channel margin on the southern side (Fig. 4B). In the lowermost 1.25 m, weakly laminated strata are ungraded or normally graded with poorly developed ripple cross-lamination. Close to the base of the unit, abundant hematite-preserved leaves (Fig. 4C and D) and seeds form discontinuous mats, which are locally penetrated by roots. Intercalated with the mats are discontinuous, disrupted lenses with slickensides and mud cracks up to 4 cm-deep, variably with or without root traces (Fig. 4E); root traces become more abundant from the channel thalweg to the margin. Also present in the mudstone close to the channel margin are charcoal fragments (Fig. 4D), indeterminate bivalves and coprolites up to 3 cm in length, provisionally attributed to fishes. The topmost 0.75 m of the lenticular unit has desiccation cracks, slickensides, a few root traces and thin lenses of ripple cross-laminated sandstone.

Red massive mudstone occurs in three additional areas. On the northern side of the outcrop belt, inclined strata rest on 1.2 m of mudstone (Fig. 4 F and G). In the lower part, grey and brown lenses of laminated claystone are separated by structureless layers with a few root traces, with thin lenses of ripple cross-laminated sandstone and siltstone above. Adjacent to the steeply-dipping channel margin on the southern side (Fig. 4A), an extensive mudstone sheet 2.6 m-thick is consolidated at the base and more friable above, with rare root traces, slickensides, clastic dikes, wedge-shaped peds and abundant redoximorphic spots. Additionally, poorly exposed outcrops of structureless mudstone also underlie channel base deposits. Petrographic analysis indicates that all occurrences of the massive mudstone are similar in composition and texture to the structureless mudstone in the inclined strata, with no mud aggregates identified.

Interpretation: The large lens of weakly laminated to structureless mudstone represents an abandoned-channel fill, with deposition from suspension and from flows charged with fine sediment. The water body supported bivalves and probably fish but periodically dried out, as indicated by the presence of disrupted layers with mud cracks (Tunbridge 1984; Smoot & Olsen 1988; Smoot 1991). Rooted vegetation grew in the channel, as indicated by relatively abundant root traces in the mudstone, especially near the southern margin. Leaves probably fell into the channel from vegetation growing within the channel and along the riparian zone and charcoal fragments indicate periodic wildfires.

The structureless mudstone sheet south of the channel margin is interpreted as floodplain deposits laid down by overbank floods. The unit below the inclined strata on the northern side is interpreted as the abandonment fill of an underlying channel body (see below).

The presence of slickensides and clastic dikes suggests that mudstone at all sites was pedogenically overprinted to form palaeosols with similar properties to Pedotype G of DiMichele *et al.* (2006), which they interpreted as a palaeo-Vertisol. Unlike other upper Clear Fork localities (Simon, 2016), massive mudstone at MR3 contains no evaporite or carbonate nodules or beds.

GEOMETRY AND EVOLUTION OF THE CHANNEL BODY

At the time of abandonment, the depth of the MR3 channel was approximately 2 m, based on the vertical extent of inclined accretion sets, which matches the thickness of the massive mudstone lens in the abandoned-channel fill (Fig. 5). The width was 36 m, with a width:depth ratio of 18. Palaeoflow was north-west (308°), determined from 46 measurements of ripple cross-lamination on the inclined surfaces (Fig. 1C).

The channel body forms the upper part of a multi-storey body. On the northern side of the outcrop belt, it rests erosively on a poorly exposed channel body with northward-dipping accretion deposits and a mudstone abandonment fill (Fig. 5). Along the channel margin on the southern side, it cuts into floodplain deposits.

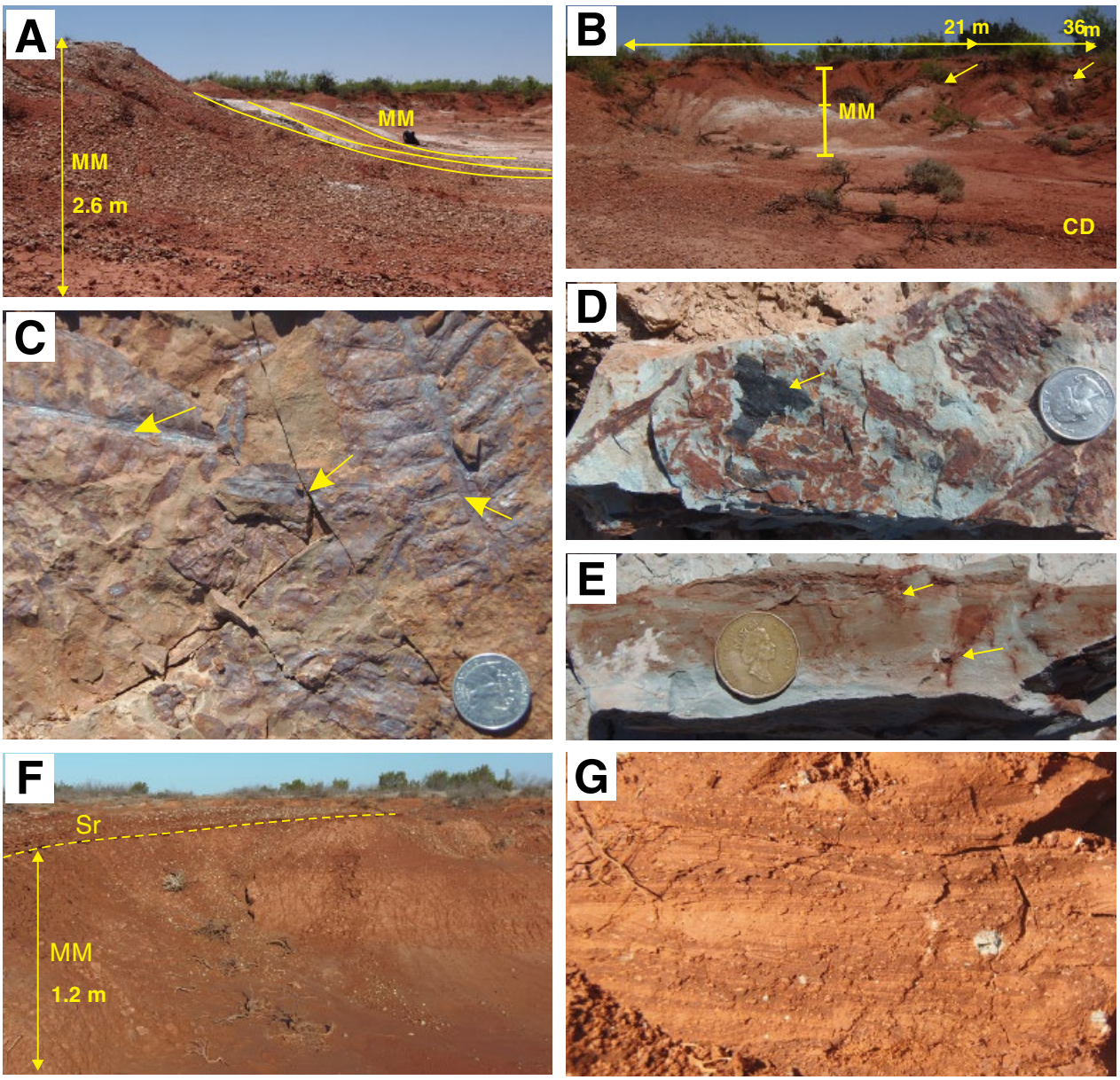

Fig. 4. Structureless mudstone (element MM). (A) Red and grey weakly laminated to structureless mudstone (MM at upper right) onlapping the steeply-dipping channel margin cut into red structureless mudstone (element MM at lower left), with rare root traces, slickensides, clastic dikes, wedge-shaped peds and abundant redoximorphic spots. (B) Abandoned channel containing concentric fill of element MM, which overlies channel-base deposits. The yellow arrows highlight the decreased width and depth of the abandoned channel as the fill advanced to the left. (C) Permineralised leaves preserved on the planes of weakly laminated mudstone with the yellow arrows highlighting the midrib of the leaves. Coin: 2.1 cm. (D) Charcoal fragments (yellow arrow) preserved alongside leaves. Coin: 2.1 cm. (E) Roots < 5 cm-long and 1 cm-wide preserved in weakly laminated mudstone, which commonly overlies the layers with plant fossils. Coin: 2.6 cm. (F/G) Structureless mudstone below the earliest recorded accretion deposit on the exhumed point bar (Sr, dipping to the north). The bed contains ripple cross-laminated sets up to 5 cm-thick with abundant redoximorphic spots.

The channel-base deposits are thin and relatively fine-grained and the carbonate clasts were derived from local palaeosols. These observations imply limited sediment availability on the alluvial plain and probably a long transport distance (Simon & Gibling, 2017a). The presence of mounds suggests that obstacles were present at the channel base, focusing sediment build-up.

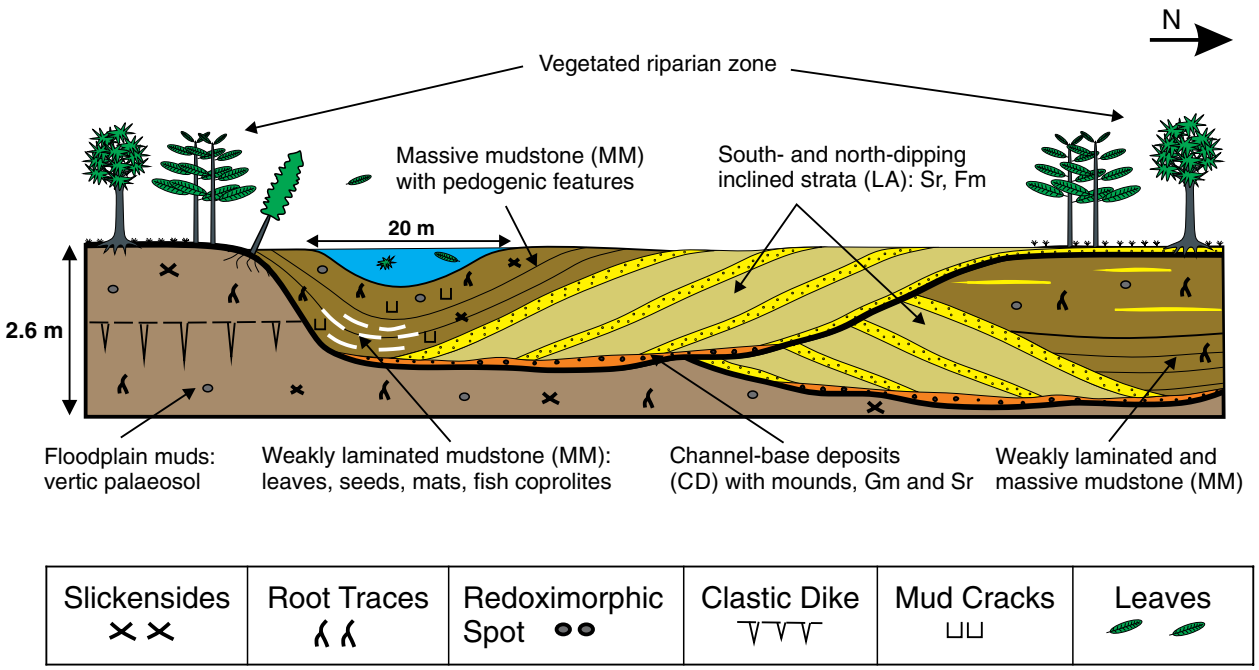

Fig. 5. Geometry, architectural elements and sedimentary features of the fine-grained meandering channel bodies at Montgomery Ranch 3 site. In the main channel body, the abandoned channel fill contains plant debris, roots and fish coprolites (not shown on the figure). Vertical scale is exaggerated.

With root traces present locally within the channel body, the obstacles may have been rooted vegetation, although no direct evidence supports this inference.

Inclined strata formed along the convex margin of a fine-grained point bar, which advanced over and in association with the basal deposits, with expansion in the dip direction. Sand was transported as bedload during the most active, near-bankfull conditions. During the final stages of these active periods, rill casts and swept ripples formed as the water-level fell. Mud was laid down during low-energy conditions with water levels approaching bankfull, as indicated by the extent of the mudstone layers from the channel base to the top of the ridges with inclined layers. Petrographic evidence supports deposition of mud largely from suspension, with no evidence of mud aggregates. Root traces within mudstone and sandstone units indicate that vegetation grew periodically within the channel.

The composite nature of many sandstone units and the probable composite nature of the thick mudstone units suggests that units of both types represent numerous flood events. The alternation of sediment types may reflect intrinsic events in the channel system, for example periodic access to a sand supply upstream. However, the correlation between lithology and flow strength suggests periodic variation in climatically controlled discharge conditions, including flood frequency and intensity, as documented on a decadal to century scale in the relatively arid south-west United States (Hereford, 2002; Harden *et al.*, 2010).

After migrating southward for at least 50 m, the channel avulsed to a new location. Water ponded within the abandoned channel where weakly laminated to structureless massive mudstone accumulated, with plant debris, bivalves and coprolites. The presence of plant beds penetrated by roots and overlain by disrupted, root-free mudstone implies that short-lived plants grew repeatedly within the channel, which was alternately water-filled then dry and exposed; some bed surfaces may represent a considerable period of time. The laminated mudstone at MR3 has a similar mineralogical composition to mudstone in other abandoned-channel fills in the formation but is generally coarser and lacks the regular, varicoloured laminae of other localities (Simon *et al.*, 2016). These differences may reflect more frequent exposure, precluding the formation and preservation of fine-scale lamination and influencing water chemistry.

An upward change to structureless mudstone, with evidence for desiccation, growth of vegetation and pedogenesis, probably represents a combination of sedimentation and drop in water level in the channel. The lithological change corresponds to a decrease in the channel width and depth to 21 m and 0.75 m, respectively. The width : depth ratio of 28, greater than the ratio of 18 at an early stage of abandonment, indicates that vertical accretion in the channel outpaced bank accretion. The preservation of a concentric fill of structureless mudstone (Fig. 4B) indicates that the channel was not reoccupied and the multi-storey body was fully abandoned in this area.

PLANT FOSSILS

Description: A flora characteristic of localities in the middle Clear Fork is preserved in the weakly laminated zones in the massive mudstone of the abandoned channel. Species richness is quite low. Three foliage taxa dominate the flora: *Evolsonia texana* (Mamay, 1989), marattialeans (possibly of more than one type) and *Taeniopteris* sp., in order of relative abundance. There are hints of other taxa represented only by scraps of foliage, possibly including pteridosperms (callipterids or medullosans) and *Sphenophyllum* sp. In addition, seeds are abundant on some bedding surfaces.

Evolsonia texana is the only species of this genus, which is attributed to the enigmatic plant family Gigantopteridaceae. The higher order affinities of the gigantopterids are probably with the seed plants, although relatedness to the Peltaspermales has been suggested (DiMichele *et al.*, 2005). The *Evolsonia* leaves are variable in size but locally large, >30 cm-long and >15 cm-wide. They are oval (Fig. 6A) with a complex, four-order venation (Fig. 6B and C); the 4th order forms an anastomosing network. The leaves were probably of stout construction with robust midvein and secondary veins (Fig. 6B and C) and vaulted between secondary veins (Fig. 6C and D).

The habit of *Evolsonia texana* is not known. Horizontally disposed axes with roots emanating from the lower side were found in a central part of the abandoned channel; the abundant *Evolsonia* leaves above this layer open the possibility that the plant may have had a ground creeping habit. The robust construction of the leaves suggests long retention times on the plant. However, gigantopterids were among the early Permian tropical plants most heavily affected by insect herbivory, typically associated with lightly built leaves that have short life spans (Glasspool *et al.*, 2003; Beck & Labandeira, 1998; Schachat *et al.*, 2014). If the leaves were relatively short-lived, *Evolsonia* may have colonised disturbed habitats and had more rapid growth rates than if it retained its leaves for an extended period.

If the gigantopterids were seed plants, their seeds have not been confidently identified. However, asymmetrical, ovoid, flattened seeds (Fig. 6E) have been found consistently in association with gigantopterid remains in American deposits. Such seeds are common at MR3 and may have been produced by *Evolsonia*.

Marattialean fern foliage occurs in dense mats locally and is closely intermixed with other plant elements, commonly on the same bedding surfaces as *Evolsonia* (Fig. 7A and D). Both sterile (Fig. 7A) and fertile foliage (Fig. 7B and C) occur in the deposit. The fertile foliage suggests that more than one species of marattialean fern is present. Although iron encrustation has contributed to poor preservation, the synangia (fused groups of sporangia, the spore-producing organs) in the specimen illustrated in Fig. 7B appear to be elongated laterally with a second type seen in Fig. 7, which is circular. Both synangial structures are known in marattialeans in Pennsylvanian and Permian floras.

Late Palaeozoic marattialeans are generally thought to have been tree ferns with their trunks supported by a mantle of adventitious roots (Morgan, 1959), a habit reported among from early Permian species of this group (Rößler, 2000). They appear to have favoured habitats with high water tables, although not necessarily flooded; their roots contain abundant air spaces (aerenchyma; Ehret & Phillips, 1977), a feature frequently associated with plants subject to occasional to frequent flooding. Marattialeans produced copious spores and were excellent colonisers. They have been reported from Permian channel belts in far western Pangea and are among those ‘wetland’ plants, along with the calamitaleans, that have the broadest distribution in space and time, colonising landscapes that were otherwise seasonally dry and moisture-limited (Naugolnykh, 2005; DiMichele *et al.*, 2006; Tabor *et al.*, 2013).

Leaves of *Taeniopteris* sp. are also present. This is a genus of uncertain affinities and may include

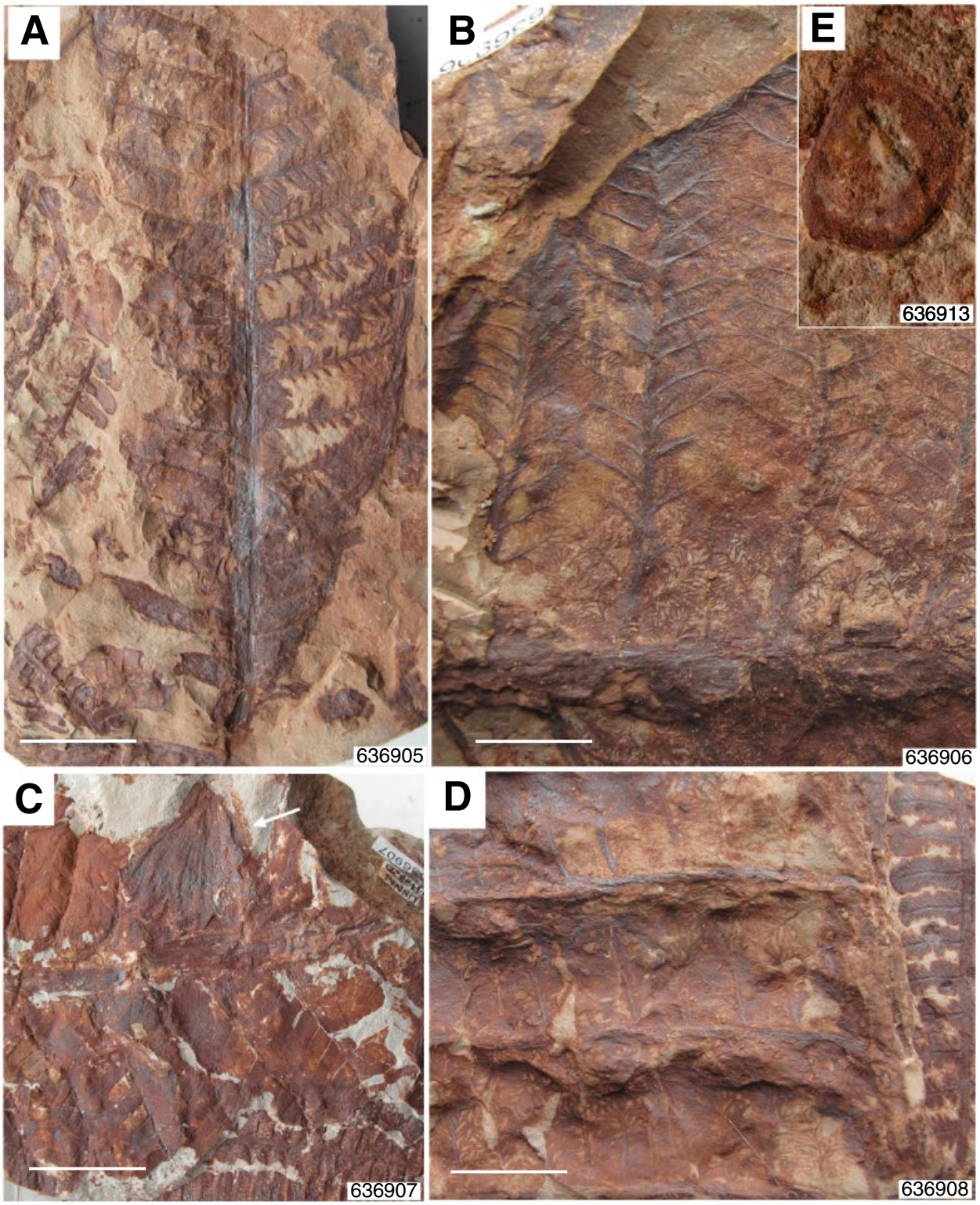

Fig. 6. *Evolsonia* from the MR3 channel body. (A) Leaf showing main architectural features of leaf shape and venation. Note co-occurring marattialean fern foliage. USNM specimen 636905. USNM locality 41382E. (B) Detail of leaf venation showing progressive size diminishment from midvein to secondary, tertiary and quaternary veins. The ultimate veins (quaternary) form a mesh. There is no suture vein, typical of some other gigantopterids. USNM specimen 636906. USNM locality 41382E. (C) Detail illustrating the three-dimensionality of the leaf surface. Note associated fertile marattialean foliage. Arrow points to an unidentified leaf, possibly *Sphenophyllum*. USNM specimen 686907. USNM locality 41382D. (D) Detail of venation; note particularly the ultimate reticulate mesh. Marattialean fern foliage in close association. USNM specimen 636908. USNM locality 41382E. (E) Asymmetrical seed of gigantopterid type. USNM specimen 636913. USNM locality 43866. Scale bars = 1 cm.

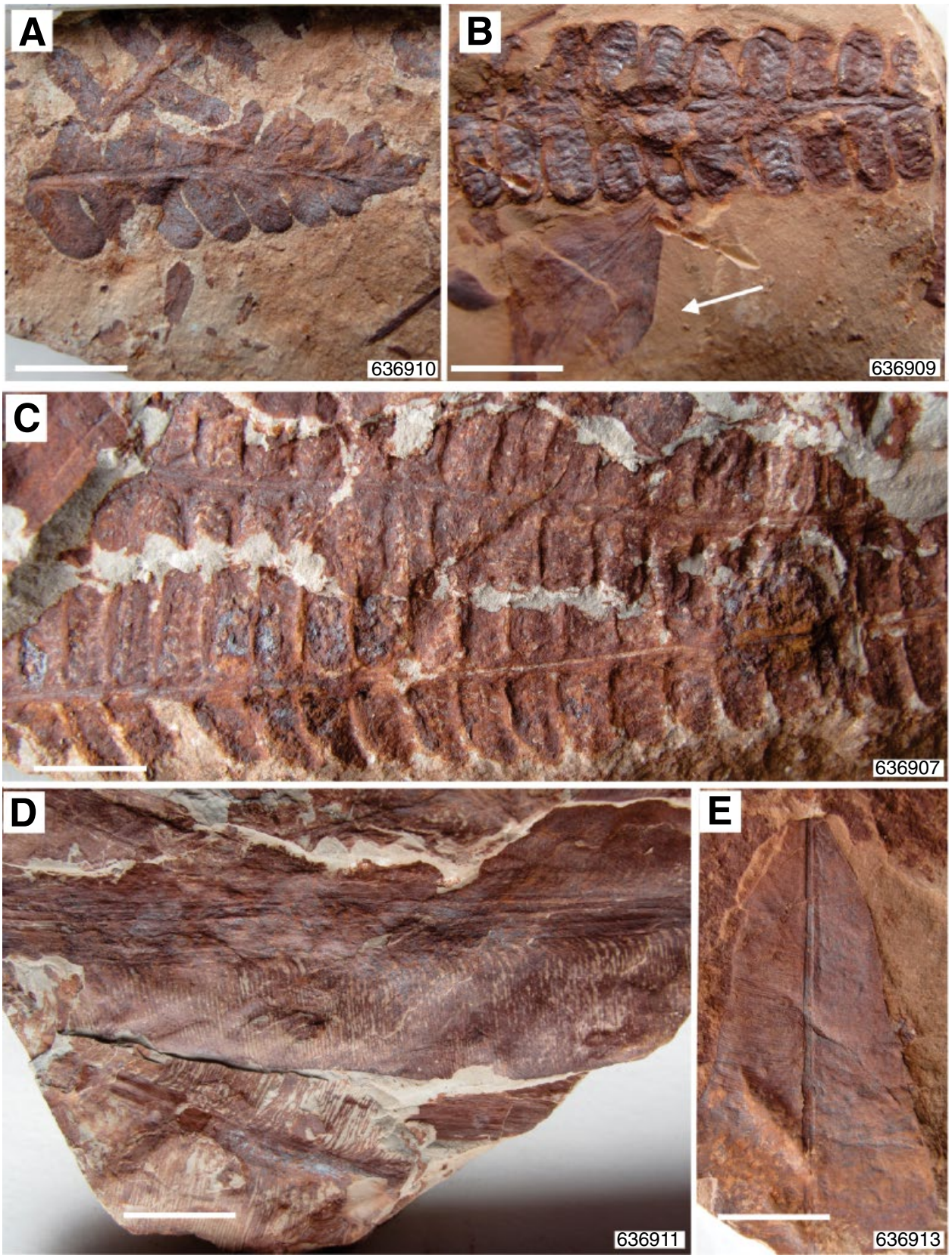

Fig. 7. Other floral elements from the MR3 channel body. (A) Sterile marattialean fern foliage. USNM specimen 636910. USNM locality 41382D. (B) Fertile marattialean fern foliage with elongate, oval synangia (Danaeites type). Arrow points to unidentified leaf, possibly *Sphenophyllum*. USNM specimen 636909. USNM locality 41382E. (C) Fertile marattialean fern foliage with round synangia (Asterotheca type). USNM specimen 636914. USNM locality 41382D. (D) *Taeniopteris* sp. Two specimens of different size illustrating basic architecture of the leaf. USNM specimen 636911. USNM locality 41382E. (E) *Taeniopteris* sp., leaf tip. USNM specimen 636912. USNM locality 41382E. Scale bars = 1 cm.

both ferns and seed plants; the taxonomy is complex and many species have been described (Remy & Remy, 1975). The larger leaves, such as those in the MR3 flora (Fig. 7D and E), are generally attributed to seed plants, possibly cycadophytes (Mamay, 1976). No reproductive organs have been found in association with these leaves.

The habit of *Taeniopteris* plants is uncertain. Whole plants with leaves attached have not been found in late Palaeozoic deposits. However, branch fragments with attached leaves are known from the western Pangean equatorial region (e.g. Koll & DiMichele, 2013) and the plant may have been a small tree. *Taeniopteris* is generally found in association with other floral elements that suggest seasonal drought, as reported from its earliest occurrence in central and western Pangea (Bashforth *et al.*, 2016).

There are indications of other kinds of plants in the MR3 assemblage, but they are represented by fragments or isolated leaves of uncertain affinity. Two such specimens are illustrated (arrows in Figs 6c and 7B). In each instance, the wedge-shaped lamina and multiple veins suggest that these may be leaves of the groundcover sphenopsid *Sphenophyllum*, perhaps of the S. *verticillatum* or S. *thonii* type.

Interpretation of life setting: Although the uncertain affinity and ecological tolerance of some taxa reduces their utility for palaeoenvironmental assessment, comparison with Pennsylvanian and early Permian assemblages across Euramerica allows a reasonable interpretation of the preferred habitat of the taxa found here. The assemblage is somewhat unusual in view of the ecological affinities broadly attributed to these plants, based on their patterns of occurrence in time and space. The assemblage includes plants typically associated with seasonal soil-moisture deficits, particularly *Evolsonia* and *Taeniopteris*, closely intermixed with plants generally associated with a persistently high water table and humid conditions, such as marattialean ferns. The ferns may have lived along the channel margin or even in parts of the channel where water levels remained high during drier seasons or periods. Marattialean foliage is not uniformly distributed in the channel deposits but, where observed, forms dense mats on bed surfaces. Overall, the flora suggests that the background conditions were seasonally dry, but that wet areas suitable for colonisation and growth of tree ferns persisted locally in or adjacent to the channel.

ADJACENT SITES MR1 AND MR2

Although in close proximity and within a stratigraphic interval of less than 50 m, the three sites at Montgomery Ranch (MR1, MR2 and MR3; Fig. 1C) display key differences, relevant to a broader landscape assessment. A summary of key features of MR1 and MR2 is given here (see Simon & Gibling, 2017a, for a fuller description).

Located 0.94 km south-west of MR3, the MR1 site has inclined beds of mudstone and sandstone with a vertical extent of 2.2 m and an average dip of 14.7 ± 4.4° (n = 27). The mudstone is structureless to weakly ripple cross-laminated with rare preservation of trough cross-beds that angled up the inclined surfaces. Petrographic analysis showed that flattened sand-sized mud aggregates are present. The sandstones include preserved dune forms at the base of the channel with crests angled up the inclined surfaces, passing updip into ripples with crests angled down the surfaces. The updip orientation of dune crests in the mudstone and sandstone indicates helicoidal flow within the channel, whereas the down-dip oriented ripple crests above suggest re-entry of overbank water into the channel when bankfull conditions were exceeded; overbank flows are also supported by the presence of thin crevasse splays in adjacent floodplain deposits. Root traces are common in the inclined layers, with a few leaves preserved close to the base of the accretion deposits. Palaeoflow was to the south-south-west (203°).

Located 1.5 km south-west of MR3 and 400 m south-west of MR1, the MR2 site has inclined sandstone beds with 2 m of vertical extent and an average dip of 13 ± 2.3° (n = 14). Trough and planar cross-sets attributed to dunes are angled up the inclined surfaces, indicating helicoidal flow. Mudstone layers are a minor component and leaves and root traces were not observed. Palaeoflow was to the west-north-west (285°).

DISCUSSION

Spectrum of channel accretion processes

All three sites (MR1, MR2 and MR3) exhibit exhumed point bars with inclined strata, with especially good planform exposure at MR3 where convex accretion surfaces face an abandoned channel and cutbank. The channels at all three

sites were of modest size, a few metres deep and a few tens of metres wide. Palaeoflow vector means are 203°, 285° and 308°, respectively and the channel bodies are inferred to represent reaches of a westerly-directed meandering-fluvial system, in accord with other localities. The channels occupied a distal position on a dryland alluvial plain where coarser sediment was limited to fine quartzose sand and carbonate clasts and mud aggregates were reworked from palaeosols. The sand was sourced from outside the basin or derived from locally stored sediment that was excavated during flood events (Simon & Gibling, 2017a,b).

Based on the criteria of Table 1, lateral accretion was the predominant process for sandstone and mudstone in the MR1 and MR2 channel bodies. Quartzose sand is relatively abundant and intercalated mudstone beds are scarce in MR2. Dune forms and large-scale cross-beds low in the channel bodies indicate bedload transport under conditions of moderate flow strength and helicoidal flow. In the mudstones at MR1, cryptic trough cross-beds with mud aggregates indicate transport of much of the mud as bedload.

In contrast, lateral accretion and oblique accretion alternated in the more mud-rich MR3 channel body (Fig. 8). In the sandstone units, dune forms and large-scale cross-beds were not observed, but ripple cross-lamination indicates bedload transport, with local erosional events. In the mudstone units, neither bedforms nor sand-sized mud aggregates were observed and mixed silt and clay suggest deposition predominantly from suspension. We infer that the sandstone units represent lateral accretion during periods of relatively strong flow, whereas the relatively thick mudstone units represent oblique accretion during longer periods of low-energy flow, when suspended sediment draped the inclined surfaces, probably during repeated flood events.

One potential criterion for distinguishing lateral from oblique accretion is the dip of the inclined surfaces (Table 1). The average dip of surfaces at MR3 is 15.6°, only slightly steeper than an average of 13° at MR1 and 14.7° at MR3. At other localities (element LA-2 of Simon & Gibling, 2017a), mud-rich inclined strata show moderate dips of 12 to 15° and, as with MR3, the mudstones were interpreted as oblique-accretion deposits on the basis of predominant silt and clay and an apparent lack of aggregates. All three Montgomery Ranch sites have relatively steep surfaces in comparison with many modern point bars (Table 1) and in the dryland setting of western Pangea, case-hardening of mud may have contributed to bank strength and steep surfaces, along with the presence of vegetation (see below).

Oblique-accretion deposits in some modern channels dip much more steeply than those at MR3, up to 29° in the Murrumbidgee River (Page

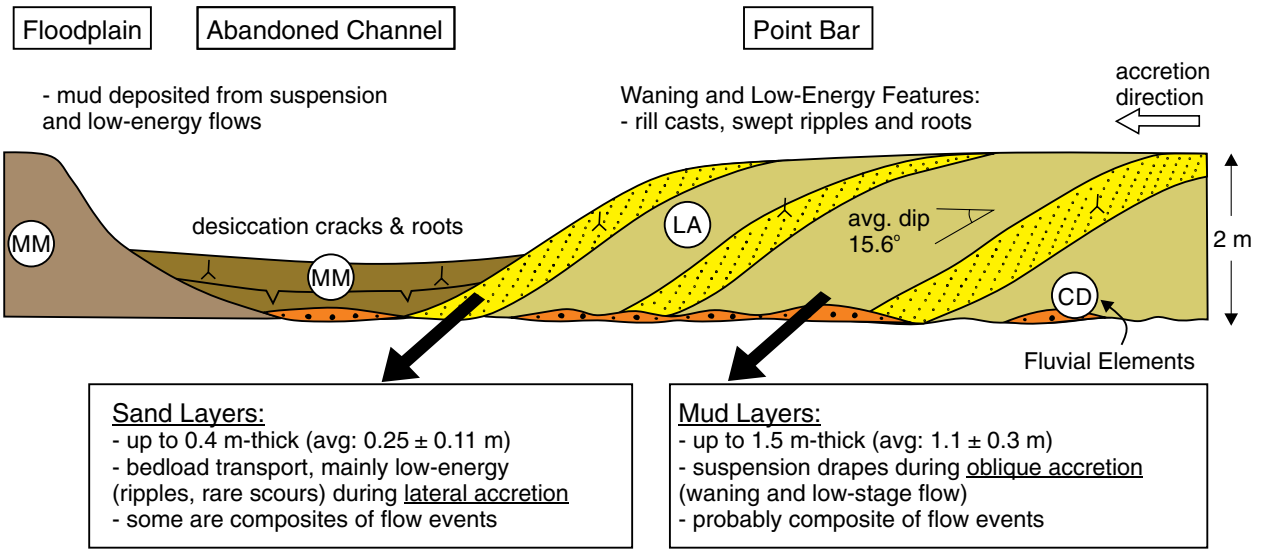

Fig. 8. Schematic diagram to show processes of mud and sand accumulation in fine-grained point bar at MR3. Within the inclined strata of the point bar, textural evidence suggests that, predominantly, the mud was laid down from suspension (oblique accretion) whereas the sand was transported as bedload (lateral accretion). The thickness of the mud layers and the observed composite nature of some sand layers suggests that they represent multiple flow events.

et al., 2003) and up to 40° in the Red River (Brooks, 2003a). The lower dips at MR3 may reflect the small dimensions and low bank height of the channel, in comparison to the Murrumbidgee (average 6 m-deep and 80 m-wide) and the Red River (up to 9.5 m-deep and 75 m-wide). Smaller modern systems with obliquely accreted mud and ripple cross-laminated sand may provide better analogues. Dips of 15° were recorded in the Channel Country of Australia (Gibling *et al.*, 1998) and dips of 8 to 12° were recorded in the upper Klip River of South Africa (Marren *et al.,* 2006), with channels in both instances 3 to 5 m-deep and 30 to 40 m-wide.

Counter point bar deposits were not identified at the three sites. As noted in Table 1, they would be expected to show concave planforms with respect to the adjacent channel and the Peace River examples described by Smith *et al.* (2009) consist mainly of rippled siltstone with upstream-directed bedforms and minimal clay.

In summary, the three Montgomery Ranch sites exhibit a spectrum of point-bar processes from predominantly lateral accretion to alternate episodes of lateral and oblique accretion. Based on the pronounced curvature of the accretion surfaces at MR3, the authors consider that the inclined strata were laid down on a point bar where mud drapes accumulated during periods of low-energy and waning flow, as on steeper accretionary banks in modern channels.

Overall, the river systems of Central Australia provide a reasonable analogue for the Montgomery Ranch sites. A supply-limited system, the Channel Country channels transport fine sediment from distant sources across a wide, low-gradient plain (Nanson & Croke, 1992; Maroulis & Nanson, 1996; Gibling *et al.,* 1998). Anabranching and avulsive channels commonly migrate slowly and fill through oblique and vertical accretion with local lateral accretion and more rapid migration. Their deposits contain quartz sand (locally recycled from the excavation of subsurface sands), sand-sized mud aggregates reworked from vertic soils, fine sediment deposited from suspension and organic material.

Water availability and contribution of vegetation to channel dynamics

The MR3 plant assemblage is dominated by gigantopterids (*Evolsonia*, a probable seed plant), marattialeans (tree ferns) and *Taeniopteris* (a possible cycadophyte, probably small trees), with other more cryptic taxa. *Evolsonia* and *Taeniopteris* are interpreted to have grown under conditions of seasonal soil-moisture deficit. *Evolsonia* may have had a creeping mode of life in the MR3 channel, although this is not certain and was capable of colonising disturbed habitats. In contrast, the marattialeans with adventitious roots and aerenchyma, could tolerate floods and preferred a high water table and high humidity, but were capable colonisers in seasonal settings.

At first sight, this habitat assessment suggests conflicting preferences for taxa in the same assemblage. A probable resolution is that the landscape was seasonally dry under semi-arid to arid conditions (Tabor & Montañez, 2004; DiMichele *et al.,* 2006), but that water was retained in wet areas of the channel and was accessible as groundwater below the channel belt for riparian water uptake, as in the Channel Country (Cendón *et al.*, 2010). Thus, taxa with different habitat tolerances could coexist within a channel reach. Demko *et al.* (1998) suggested that dryland valley fills would be biased towards riparian wetland habitats and Simon *et al.* (2016) suggested that moisture persisted locally in an oxbow lake, promoting plant growth and preservation on the Clear Fork dryland plain.

An initial reconnaissance might suggest that vegetation contributed little to channel dynamics in this early Permian formation. Upright trees and large logs are absent from the Montgomery Ranch sites and very rare in the formation as a whole and plant fossils are sparse and commonly poorly preserved. However, the excavation of exceptional plant-fossil localities over many years, especially in abandoned-channel fills (DiMichele *et al.*, 2006; Looy, 2013; Simon *et al.*, 2016), shows that a range of taxa was present near the channels, including trees with large leaves (Fig. 5). Examination of sandstone and mudstone beds shows that roots are widespread within the channel bodies and along their margins. These observations indicate that vegetation must be taken into account in assessing channel morphodynamics, although analysis will be largely qualitative.

As in modern settings and in ancient examples (Rygel *et al.*, 2004; Ielpi *et al.*, 2015), vegetation probably contributed significantly to bank stabilisation, along with abundant cohesive mud that would have hardened in the relatively arid setting (Gibling *et al.*, 1998; Matsubara *et al.*, 2015). With evidence for rooted vegetation within the MR3

channel, upright vegetation (especially of disturbance-tolerant taxa such as *Evolsonia* and marattialeans) and transported plant material may have nucleated sediment accumulation. No hard evidence for this was found at MR3 but wood fragments are present in channel-base mounds at other sites (Simon & Gibling, 2017a). The MR3 channel may have provided an especially suitable habitat for plant growth in view of the prolonged low-energy periods during point-bar migration, standing water following floods (as indicated by symmetric ripples) and standing water in the abandoned channel. Finally, a well-developed riparian zone would have promoted animal life, including the tetrapods for which the formation is famous.

CONCLUSIONS

A crucial issue in studying fine-grained meandering channels is to establish the processes that laid down the mud. This requires analysis of outcrop features and microscopic textures, both of which are probably cryptic and modified by weathering and diagenesis. In the early Permian Clear Fork Formation at Montgomery Ranch site MR3, exhumed point-bar deposits of a small channel (2 m-deep and 36 m-wide) comprise alternate, thin (<0.4 m) units of quartzose sandstone and thick (<1.5 m) of mudstone, laid down under a relatively arid climate. The sand was transported as bedload during active flow and the mud was laid down as suspension drapes of silt and clay that covered the inclined point-bar surfaces (with an average dip of nearly 16°) during waning and low-stage flow. Sand-sized mud aggregates and cryptic bedforms are present in channel mudstones elsewhere in the formation but, despite a careful search, were not identified in the MR3 mudstones, strengthening the case for deposition of mud from suspension rather than bedload. Thus, alternate periods of lateral accretion and oblique accretion were involved in the construction of the point bar (Fig. 8). Both sandstone and mudstone units are composites of numerous flows, suggesting a link to climatically controlled secular variation in discharge and flood parameters.

Plant fossils are generally scarce in the formation and may easily be overlooked in assessing channel dynamics. However, an associated abandoned-channel fill at MR3 contains an assemblage of gigantopterids (*Evolsonia texana*), marattialean foliage and *Taeniopteris* sp. Root traces penetrate the leaves and are also present in the point-bar deposits. These observations suggest that, under conditions of seasonal flow in the channel system, vegetation grew widely in the channels and on the banks, with some taxa exploiting wetter sites in an otherwise moisture-deficient setting. The vegetation may have been sufficiently abundant to influence channel processes and geometry, although direct evidence is lacking. Fine-grained channels under a seasonal flow regime but with periodic standing water and wetter reaches, may be especially well suited to the establishment of vegetation.

ACKNOWLEDGEMENTS

The authors thank John Holbrook and Colin North for thoughtful reviews that greatly helped in focusing the manuscript. We thank James Edwards of Montgomery Ranch for property access to the outcrops. Thin sections were prepared at Dalhousie University by Gordon Brown and by Vancouver Petrographics Limited. The authors thank Georgia Pe-Piper and Xiang Yang at Saint Mary's University for assistance with SEM analysis and David Piper, Owen Brown, Lori Campbell and Jenna Higgins at Bedford Institute of Oceanography for assistance with X-ray diffraction. The authors are especially grateful to Neil Tabor, Timothy Myers and Lu Zhu for logistical support. Research was funded by a Discovery Grant to Martin Gibling from the Natural Sciences and Engineering Research Council of Canada (NSERC) and by research grants to Sharane Simon from the Society for Sedimentary Geology (SEPM) and Geological Society of America (GSA).

REFERENCES

Allen, J.R.L. (1970) Studies in fluviatile sedimentation: A comparison of fining upwards cyclothems with special reference to coarse-member composition and interpretation. *J. Sed. Petrol.*, **40**, 298–323.

Anderson, J.S., **Reisz, R.R.**, **Scott, D.**, **Frobisch, N.B.** and **Sumida, S.S.** (2008) A stem batrachian from the Early Permian of Texas and the origin of frogs and salamanders. *Nature*, **453**, 515–518.

Bashforth, A.R., **Cleal, C.J.**, **Gibling, M.R.**, **Falcon-Lang, H.J.** and **Miller, R.F.** (2014) Paleoecology of Early Pennsylvanian vegetation on a seasonally dry tropical landscape (Tynemouth Creek Formation, New Brunswick, Canada. *Review of Palaeobotany and Palynology*, **200**, 229–263.

Bashforth, A.R., **DiMichele, W.A.**, **Eble, C.F.** and **Nelson, W.J.** (2016) Dryland vegetation from the Middle Pennsylvanian of Indiana (Illinois Basin): the dryland biome in glacioeustatic, paleobiogeographic and paleoecologic context. *J. Paleontol.*, **90**, 785–814.

Beck, A.L. and **Labandeira, C.C.** (1998) Early Permian insect folivory on a gigantopterid-dominated riparian flora from north-central Texas. *Palaeogeogr., Palaeoclimatol., Palaeoecol.*, **142**, 139–173.

Bein, A. and **Land, L.S.** (1983) Carbonate sedimentation and diagenesis associated with Mg-Ca-chloride brines; the Permian San Andres Formation in the Texas Panhandle. *J. Sed. Res.*, **53**, 243–260.

Bluck, B. (1971) Sedimentation in the meandering River Endrick. *Scot. J. Geol.*, **7**, 93–138.

Brister, B.S., **Stephens, W.C.** and **Norman, G.A.** (2002) Structure, stratigraphy and hydrocarbon system of a Pennsylvanian pull-apart basin in north-central Texas. *AAPG Bull.*, **86**, 1–20.

Brooks, G.R. (2003a) Alluvial deposits of a mud-dominated stream: the Red River, Manitoba, Canada. *Sedimentology*, **50**, 441–458.

Brooks, G.R. (2003b) Holocene lateral channel migration and incision of the Red River, Manitoba, Canada. *Geomorphology*, **54**, 197–215.

Budnik, R.T. (1989) *Tectonic structures of the Palo Duro Basin, Texas Panhandle*. Bureau of Economic Geology, University of Texas, Austin, 43 p.

Cendón, D.I., **Larsen, J.R.**, **Jones, B.G.**, **Nanson, G.C.**, **Rickleman, D.**, **Hankin, S.I.**, **Pueyo, J.J.** and **Maroulis, J.** (2010) Freshwater recharge into a shallow saline groundwater system, Cooper Creek floodplain, Queensland, Australia. *J. Hydrol*, **392**, 150–163.

Chaney, D.S. and **DiMichele, W.A.** (2007) Paleobotany of the classic redbeds (Clear Fork Group – Early Permian) of north-central Texas. In: *Proc. XVth Int. Cong. Carb. Perm. Strat.* (Ed. T.E. Wong), pp. 357–366. University of Utrecht, The Netherlands.

DiMichele, W.A., **Kerp, H.**, **Krings, M.** and **Chaney, D.S.** (2005) The Permian peltasperm radiation: evidence from the southwestern United States. *New Mex. Mus. Nat. Hist. Sci. Bull.*, **30**, 67–79.

DiMichele, W.A., **Tabor, N.J.**, **Chaney, D.S.** and **Nelson, W.J.** (2006) From wetlands to wet spots: Environmental tracking and the fate of carboniferous elements in Early Permian tropical floras. In: *Wetlands through Time*. (Eds S.F. Greb and W.A. DiMichele), *Geol. Soc. Am. Spec. Publ.*, **399**, 223–248.

Edmaier, K., **Burlando, P.** and **Perona, P.** (2011) Mechanisms of vegetation uprooting by flow in alluvial non-cohesive sediment. *Hydro. Earth Syst. Sci.*, **15**, 1615–1627.

Edwards, M.B., **Eriksson, K.A.** and **Kier, R.S.** (1983) Paleochannel geometry and flow patterns determined from exhumed Permian point bars in north-central Texas. *J. Sed. Res.*, **53**, 1261–1270.

Ehret, D.L. and **Phillips, T.L.** (1977) *Psaronius* root systems — morphology and development. *Palaeontographica Abteilung B*, **161**, 147–164.

Èkes, C. (1993) Bedload-transported pedogenic mud aggregates in the Lower Old Red Sandstone in southwest Wales. *Geol. Soc. Lon, J*, **150**, 469–471.

Fielding, C.R. and **Alexander, J.** (2001) Fossil trees in ancient fluvial channel deposits: evidence of seasonal and longer-term climatic variability. *Palaeogeogr. Palaeoclimatol. Palaeoecol.*, **170**, 59–80.

Fielding, C.R., **Allen, J.P.**, **Alexander, J.** and **Gibling, M.R.** (2009) A facies model for fluvial systems in the seasonal tropics and subtropics. *Geology*, **37**, 623–626.

Gastaldo, R.A., **Pludow, B.A.** and **Neveling, J.** (2013) Mud aggregates from the Katberg Formation, South Africa: additional evidence for Early Triassic degradational landscapes. *J. Sed. Res.*, **83**, 531–540.

Ghinassi, M., **Nemec, W.**, **Aldinucci, M.**, **Nehyba, S.**, **Özaksoy, V.** and **Fidolini, F.** (2014) Plan-form evolution of ancient meandering rivers reconstructed from longitudinal outcrop sections. *Sedimentology*, **61**, 952–977.

Ghosh, P., **Sarkar, S.** and **Maulik, P.** (2006) Sedimentology of a muddy alluvial deposit: Triassic Denwa Formation, *India. Sed. Geol.*, **191**, 3–36.

Gibling, M.R., **Nanson, G.C.** and **Maroulis, J.C.** (1998) Anastomosing river sedimentation in the Channel Country of central Australia. *Sedimentology*, **45**, 595–619.

Glasspool, I., **Hilton, J.**, **Collinson, M.** and **Wang, S.J.** (2003) Foliar herbivory in late Palaeozoic Cathaysian gigantopterids. *Rev. Palaeobot. Palynol.*, **127**, 125–132.

Hackley, P.C., **Guevara, E.H.**, **Hentz, T.F.** and **Hook, R.W.** (2009) Thermal maturity and organic composition of Pennsylvanian coals and carbonaceous shales, north-central Texas: Implications for coalbed gas potential. *Int. J. Coal Geol.*, **77**, 294–309.

Harden, T., **Macklin, M.G.** and **Baker, V.R.** (2010) Holocene flood histories in south-western USA. *Earth Surf. Proc. Landforms*, **35**, 707–716.

Hereford, R. (2002) Valley-fill alluviation during the Little Ice Age (ca. A.D. 1400–1880), Paria River basin and southern Colorado Plateau, United States. *Geol. Soc. Am. Bull.*, **114**, 1550–1563.

Hickin, E.J. (1979) Concave-bank benches on the Squamish River, British Columbia, *Canada. Can. J. Earth Sci.*, **16**, 200–203.

Houseknecht, D.W. (1983) Tectonic-sedimentary evolution of the Arkoma Basin and guidebook to deltaic facies, Hartshorne sandstone. *SEPM Midcontinent Section*, **1**, 3–52.

Ielpi, A. and **Ghinassi, M.** (2014) Planform architecture, stratigraphic signature and morphodynamics of an exhumed Jurassic meander plain (Scalby Formation, Yorkshire, UK). *Sedimentology*, **61**, 1923–1960.

Ielpi, A., **Gibling, M.R.**, **Bashforth, A.R.** and **Dennar, C.I.** (2015) Impact of vegetation on Early Pennsylvanian fluvial channels: insight from the Joggins Formation of Atlantic Canada. *J. Sed. Res.*, **85**, 999–1018.

Jackson, R.G., II (1976) Depositional model of point bars in the lower Wabash River. *J. Sed. Res.*, **46**, 579–594.

Jackson, R.G., II (1981) Sedimentology of muddy fine-grained channel deposits in meandering streams of the American Middle West. *J. Sed. Petrol.*, **51**, 1169–1192.

King, P.B. 1937. Geology of the Marathon region, Texas. *U.S. Geol. Surv., Prof. Pap.*, **187**, 148 p.

Koll, R. and **DiMichele, W.A.** (2013) A broad-leaved plant from the Abo Formation of northern New Mexico:

Lazarus taxon, paleobiogeographic anomay or convergent evolution? *New Mex. Mus. Nat. Hist. Sci. Bull.*, **60**, 175–177.

Looy, C.V. (2013) Natural history of a plant trait: branch-system abscission in Paleozoic conifers and its environmental, autecological and ecosystem implications in a fire-prone world. *Paleobiology*, **39**, 235–252.

Lucas, S.G., **Voigt, S.**, **Lerner, A.J.** and **Nelson, W.J.** (2011) Late Early Permian continental ichnofauna from Lake Kemp, north-central Texas, USA. *Palaeogeogr. Palaeoclimatol. Palaeoecol.*, **308**, 395–404.

Mack, G.H., **Leeder, M.R.**, **Perez-Arlucea, M.** and **Bailey, B.D.J.** (2003) Early Permian silt-bed fluvial sedimentation in the Orogrande basin of the Ancestral Rocky Mountains, New Mexico, *USA. Sed. Geol.*, **160**, 159–178.

Makaske, B. and **Weerts, H.J.T.** (2005) Muddy lateral accretion and low stream power in a sub-recent confined channel belt, Rhine-Meuse delta, central Netherlands. *Sedimentology*, **52**, 651–668.

Mamay, S.H. (1989) *Evolsonia*, a new genus of Gigantopteridaceae from the Lower Permian Vale Formation, north-central Texas. *Am. J. Bot.*, **76**, 1299–1311.

Mamay, S.H. (1976) Paleozoic origin of the cycads. *U.S. Geol. Surv. Prof. Pap.*, **934**, 1–48.

Maroulis, J.C. and **Nanson, G.C.** (1996) Bedload transport of aggregated muddy alluvium from Cooper creek, central Australia: A flume study. *Sedimentology*, **43**, 771–790.

Marren, P.M., **McCarthy, T.S.**, **Tooth, S.**, **Brandt, D.**, **Stacey, G.G.**, **Leong, A.** and **Spottiswoode, B.** (2006) A comparison of mud- and sand-dominated meanders in a downstream coarsening reach of the mixed bedrock-alluvial Klip River, eastern Free State, South Africa. *Sed. Geol.*, **190**, 213–226.

Matsubara, Y., **Howard, A.D.**, **Burr, D.M.**, **Williams, R.M.E.**, **Dietrich, W.E.** and **Moore, J.M.** (2015) River meandering on Earth and Mars: A comparative study of Aeolis Dorsa meanders, Mars and possible terrestrial analogs of the Usuktuk River, AK and the Quinn River, NV. *Geomorphology*, **240**, 102–120.

Miall, A.D. (1996) *The geology of fluvial deposits: sedimentary facies, basin analysis and petroleum geology*. Springer, Berlin.

Millar, R.G. (2000) Influence of bank vegetation on alluvial channel patterns. *Water Resour. Res.*, **36**, 1109–1118.

Milner, A.R. and **Schoch, R.R.** (2013) *Trimerorhachis* (Amphibia: Temnospondyli) from the Lower Permian of Texas and New Mexico: cranial osteology, taxonomy and biostratigraphy. *N. J. Geol. Paläontol. Ab.*, **270**, 91–128.

Morgan, E.J. (1959) The morphology and anatomy of American species of the genus *Psaronius*. *Illinois Biol. Monogr.*, **27**, 1–108.

Müller, R., **Nysuten, J.P.** and **Wright, V.P.** (2004) Pedogenic mud aggregates and paleosol development in ancient dryland river systems: criteria for interpreting alluvial mudrock origin and floodplain dynamics. *J. Sed. Res.*, **74**, 537–551.

Murry, P.A. and **Johnson, G.D.** (1987) Clear Fork vertebrates and environments from the Lower Permian of north-central Texas. *Tex. J. Sci.*, **39**, 253–266.

Nanson, G.C. and **Croke, J.C.** (1992) A genetic classification of floodplains. *Geomorphology*, **4**, 459–486.

Nanson, G.C. and **Page, K.J.** (1983) Lateral accretion of fine-grained concave benches on meandering rivers. In: *Modern and Ancient Fluvial Systems* (Eds J. Collinson and J. Lewin), *Int. Assoc. Sedimentol. Spec. Publ.*, **6**, 133–143.

Naugolnykh, S.V. (2005) Permian *Calamites gigas* Brongniart, 1828: The morphological concept, paleoecology and implications. *Paleontol. J.*, **39**, 321–332.

Nelson, W.J. and **Hook, R.W.** (2005) Pease River Group (Leonardian-Guadalupian) of Texas: an overview. *New Mex. Mus. Nat. Hist. Sci. Bull.*, **30**, 243–250.

Nelson, W.J., **Hook, R.W.** and **Chaney, D.S.** (2013) Lithostratigraphy of the Lower Permian (Leonardian) Clear Fork Formation of north-central Texas. In: *The Carboniferous-Permian Transition* (Eds S.G. Lucas, **W.A. DiMichele**, J.E. Barrick, J.W. Schneider and J.A. Spielmann), *New Mexico Mus. Nat. Hist. Sci. Bull.*, **60**, 286–311.

Olson, E.C. (1958) Fauna of the Vale and Choza: 14. Summary, review and integration of the geology and the faunas. *Fieldiana Geol.*, **10**, 397–448.

Oriel, S.S., **McKee, E.D.** and **Crosby, E.J.** (1967) Paleotectonic investigations of the Permian system in United States. *US Geol. Surv. Prof. Pap.*, Washington, U.S., 2330–7102.

Page, K.J. and **Nanson, G.C.** (1982) Concave-bank benches and associated floodplain formation. *Earth Surf. Proc. Land.*, **7**, 529–543

Page, K.J., **Nanson, G.C.** and **Frazier, P.S.** (2003) Floodplain formation and sediment stratigraphy resulting from oblique accretion on the Murrumbidgee River, Australia. *J. Sed. Res.*, **73**, 5–14.

Parker, G., **Shimizu, Y.**, **Wilkerson, G.B.**, **Eke, E.C.**, **Abad, J.D.**, **Lauer, J.W.**, **Paola, C.**, **Dietrich, W.E.** and **Voller, V.R.** (2011) A new framework for modeling the migration of meandering rivers. *Earth Surf. Proc. Land.*, **36**, 70–86.

Regan, T.R. and **Murphy, P.J.** (1986) *Faulting in the Matador uplift area, Texas: Topical Report*. Stone and Webster Engineering Corp., Boston, MA.

Remy, W. and **Remy, R.** (1975) Beiträge zur Kenntnis des Morpho-Genus *Taeniopteris* Brongniart. *Argumenta Palaeobotanica*, **4**, 31–37.

Romer, A.S. (1928) Vertebrate faunal horizons in the Texas Permo-Carboniferous red beds. *Univ. Texas Bull.*, **2801**, 67–108.

Rößler, R. (2000) The late Palaeozoic tree fern *Psaronius*—an ecosystem unto itself. *Rev. Palaeobot. Palynol.*, **108**, 55–74.

Rust, B.R. and **Nanson, G.C.** (1989) Bedload transport of mud as pedogenic aggregates in modern and ancient rivers. *Sedimentology*, **36**, 291–306.

Rygel, M.C. and **Gibling, M.R.** (2006) Natural geomorphic variability recorded in a high-accommodation setting: fluvial architecture of the Pennsylvanian Joggins Formation of Atlantic Canada. *J. Sed. Petrol.*, **76**, 1230–1251.

Rygel, M.C., **Gibling, M.R.** and **Calder, J.H.** (2004) Vegetation-induced sedimentary structures from fossil forests in the Pennsylvanian Joggins Formation, Nova Scotia. *Sedimentology*, **51**, 531–552.

Sambrook Smith, G.H., **Best, J.L.**, **Leroy, J.Z.** and **Orfeo, O.** (2016) The alluvial architecture of a suspended sediment dominated meandering river: the Río Bermejo, Argentina. *Sedimentology*, **63**, 1187–1208.

Schachat, S.R., **Labandeira, C.C.**, **Gordon, J.**, **Chaney, D.**, **Levi, S.**, **Halthore, M.N.** and **Alvarez, J.** (2014) Plant-insect interactions from early Permian (Kungurian) Colwell Creek Pond, north-central Texas: the early spread of herbivory in riparian environments. *Int. J. Plant. Sci.*, **175**, 855–890.

Scotese, C.R. (1999) PALEOMAP Animations 'Paleogeography'. In: *PALEOMAP Project*. Department of Geology, University of Texas, Arlington, TX.

Simon S.S.T. (2016) Sedimentology of the Fluvial Systems of the Clear Fork Formation in North-Central Texas: Implications for Early Permian Paleoclimate and Plant Fossil Taphonomy. Published PhD thesis, Dalhousie University, Halifax, Canada, 310 p.

Simon, S.S.T. and **Gibling, M.R.** (2017a) Fine-grained meandering systems of the Lower Permian Clear Fork Formation of north-central Texas, USA: Lateral and oblique accretion on an arid plain. *Sedimentology*, **64**, 714–746.

Simon, S.S.T. and **Gibling, M.R.** (2017b) Pedogenic mud aggregates preserved in a fine-grained meandering channel in the Lower Permian Clear Fork Formation, north-central Texas, U.S.A. *J. Sed. Res.*, **87**, 230–252.

Simon, S.S.T, **Gibling, M.R.**, **DiMichele, W.A.**, **Chaney, D.S.**, **Looy, C.V.** and **Tabor, N.J.** (2016) An abandoned-channel fill with exquisitely preserved plants in redbeds of the Clear Fork Formation, Texas, USA: an Early Permian water-dependent habitat on the arid plains of Pangea. *J. Sed. Res.*, **86**, 944–964.

Smith, D.G., **Hubbard, S.M.**, **Leckie, D.A.** and **Fustic, M.** (2009) Counter point bar deposits: lithofacies and reservoir significance in the meandering modern Peace River and ancient McMurray Formation, Alberta, Canada. *Sedimentology*, **56**, 1655–1669.

Smoot, J.P. (1991) Sedimentary facies and depositional environments of early Mesozoic Newark Supergroup basins, eastern North America. *Palaeogeogr. Palaeoclimatol. Palaeoecol.*, **84**, 369–423.

Smoot, J.P. and **Olsen, P.E.** (1988) Massive mudstones in basin analysis and paleoclimatic interpretation of the Newark Supergroup. In: *Triassic-Jurassic rifting, continental breakup and the origin of the Atlantic Ocean and passive margins* (Ed. W. Manspeizer), Elsevier, New York, 249–274.

Stewart, D.J. (1981) A meander-belt sandstone of the Lower Cretaceous of southern England. *Sedimentology*, **28**, 1–20.

Tabor, N.J. (2013) Wastelands of tropical Pangea: high heat in the Permian. *Geology*, **41**, 623–624.

Tabor, N.J., **DiMichele, W.A.**, **Montañez, I.P.** and **Chaney, D.S.** (2013) Late Paleozoic continental warming of a cold tropical basin and floristic change in western Pangea. *Int. J. Coal. Geol.*, **119**, 177–186.

Tabor, N.J. and **Montañez, I.P.** (2004) Morphology and distribution of fossil soils in the Permo-Pennsylvanian Wichita and Bowie Groups, north-central Texas, USA: implications for western equatorial Pangean palaeoclimate during icehouse-greenhouse transition. *Sedimentology*, **51**, 851–884.

Tabor, N.J. and **Poulsen, C.J.** (2008) Palaeoclimate across the Late Pennsylvanian-Early Permian tropical palaeolatitudes: a review of climate indicators, their distribution and relation to palaeophysiographic climate factors. *Palaeogeogr. Palaeoclimatol. Palaeoecol.*, **268**, 293–310.

Taylor, G. and **Woodyer, K.D.** (1978) Bank deposition in suspended-load streams. In: *Can. Soc. Petrol. Geol. Mem.* (Ed. A.D. Miall), **5**, 257–275.

Thomas, R.G., **Smith, D.G.**, **Wood, J.M.**, **Visser, J.**, **Calverley-Range, E.A.** and **Koster, E.H.** (1987) Inclined heterolithic stratification-terminology, description, interpretation and significance. *Sed. Geol.*, **53**, 123–179.

Tunbridge, I.P. (1984) Facies model for a sandy ephemeral stream and clay playa complex the Middle Devonian Trentishoe Formation of North Devon, U.K. *Sedimentology*, **31**, 697–715.

Wardlaw, B. (2005) Age assignment of the Pennsylvanian-Early Permian succession of north central Texas. *Permophiles*, **46**, 21–22.

Willis, B.J. (1989) Palaeochannel reconstructions from point bar deposits: a three-dimensional perspective. *Sedimentology*, **36**, 757–766.

Wolela, A.M. and **Gierlowski-Kordesch, E.H.** (2007) Diagenetic history of fluvial and lacustrine sandstones of the Hartford Basin (Triassic–Jurassic), Newark Supergroup, USA: *Sed. Geol.*, **197**, 99–126.

Woodyer, K.D. (1975) Concave-bank benches on the Barwon River, N.S.W. *Aust. Geogr.*, **13**, 36–40.

Ziegler, A.M., **Hulver, M.L.** and **Rowley, D.B.** (1997) Permian world topography and climate. In: *Late glacial and postglacial environmental changes: Pleistocene, Carboniferous-Permian and Proterozoic* (Ed. I.P. Martini), Oxford University Press, Oxford, 111–146.